Journal of Visualized Experiments

Methods to analyze size, shape and directionality of networks of coupled astrocytes

--Manuscript Draft--

Article Type:	Methods Article - JoVE Produced Video
Manuscript Number:	JoVE58116R2
Full Title:	Methods to analyze size, shape and directionality of networks of coupled astrocytes
Keywords:	Astrocyte networks, gap junction, patch clamp, biocytin, vectorial analysis, anatomical organization, brainstem
Corresponding Author:	Steven Condamine Université de Montréal Montreal, QC CANADA
Corresponding Author's Institution:	Université de Montréal
Corresponding Author E-Mail:	s.condamine@gmail.com
Order of Authors:	Steven Condamine
	Dorly Verdier
	Arlette Kolta
Additional Information:	
Question	**Response**
Please indicate whether this article will be Standard Access or Open Access.	Standard Access (US$2,400)
Please indicate the **city, state/province, and country** where this article will be **filmed**. Please do not use abbreviations.	Pavillon Paul-G Desmarais, bureau 5201, 2960, chemin de la Tour, Montréal (QC) H3T 1J4

Powered by Editorial Manager® and ProduXion Manager® from Aries Systems Corporation

Université de Montréal

05 March 2018

Dr Ronald Myers
Editor

Dear Dr Myers

We are submitting this article entitled "***Methods to analyse size, shape and directionality of networks of coupled astrocytes***" in the hope that you will find it acceptable for publication in *Journal of Visualized experiments*.

My colleagues and I believe that this method article should be published in the *Journal of Visualized experiments* because the subject is of interest to a wide readership. The number of functions in the brain that are thought to depend on astrocyte-neurons interactions increases constantly, and the concept that astrocytes modulate neuronal function at the network level is slowly emerging. However, no methods have been proposed so far to characterize the anatomical organization of astrocytic networks. We believe these tools will become interesting not only to characterize astrocytic networks in a defined area, but to compare networks of different areas and under different conditions.

We hope that you will find our methods of interest and consider their publication in *JoVE.*

Correspondence should be addressed to Arlette Kolta at the address and numbers given below.

Sincerely,

Arlette Kolta, PhD.

Pavillon Paul Desmarais
C.P. 6128, succursale Centre-ville
Montréal (Québec) H3C 3J7
Phone: (514) 343-7112
e-mail: arlette.kolta@umontreal.ca

Manuscript Click here to download Manuscript 58116_R2_RE.docx

TITLE:

Analyzing the Size, Shape, and Directionality of Networks of Coupled Astrocytes

AUTHORS AND AFFILIATIONS:

Steven Condamine[1], Dorly Verdier[1], Arlette Kolta[1, 2]

[1]Groupe de Recherche sur le Système Nerveux Central, and Département de Neurosciences Université de Montréal, C.P. 6128, succursale Centre-ville, Montréal, Québec, Canada, H3C 3J7

[2]Faculté de Médecine Dentaire, Université de Montréal, C.P. 6128, succursale Centre-ville, Montréal, Québec, Canada, H3C 3J7

Corresponding Author:

Arlette Kolta (arlette.kolta@umontreal.ca)

Email Addresses of Co-Authors:

Steven Condamine (steven.condamine@umontreal.ca)

Dorly Verdier (dorly.verdier@umontreal.ca)

KEYWORDS:

Astrocytes, coupling, networks, vectorial analysis, biocytin, preferential orientation, anatomical organization

SUMMARY:

Here we present a protocol to assess the organization of astrocytic networks. The described method minimizes bias to provide descriptive measures of these networks such as cell count, size, area, and position within a nucleus. Anisotropy is assessed with a vectorial analysis.

ABSTRACT:

It has become increasingly clear that astrocytes modulate neuronal function not only at the synaptic and single-cell levels, but also at the network level. Astrocytes are strongly connected to each other through gap junctions and coupling through these junctions is dynamic and highly regulated. An emerging concept is that astrocytic functions are specialized and adapted to the functions of the neuronal circuit with which they are associated. Therefore, methods to measure various parameters of astrocytic networks are needed to better describe the rules governing their communication and coupling and to further understand their functions.

Here, using the image analysis software (*e.g.*, ImageJFIJI), we describe a method to analyze confocal images of astrocytic networks revealed by dye-coupling. These methods allow for 1) an automated and unbiased detection of labeled cells, 2) calculation of the size of the network, 3) computation of the preferential orientation of dye spread within the network, and 4) repositioning of the network within the area of interest.

This analysis can be used to characterize astrocytic networks of a particular area, compare networks of different areas associated to different functions, or compare networks obtained

under different conditions that have different effects on coupling. These observations may lead to important functional considerations. For instance, we analyze the astrocytic networks of a trigeminal nucleus, where we have previously shown that astrocytic coupling is essential for the ability of neurons to switch their firing patterns from tonic to rhythmic bursting[1]. By measuring the size, confinement, and preferential orientation of astrocytic networks in this nucleus, we can build hypotheses about functional domains that they circumscribe. Several studies suggest that several other brain areas, including the barrel cortex, lateral superior olive, olfactory glomeruli, and sensory nuclei in the thalamus and visual cortex, to name a few, may benefit from a similar analysis.

INTRODUCTION:

Many studies have described how the neuron-astrocyte dialogue at a sub-cellular or synaptic level can have implications in neuronal functions and synaptic transmission. It is well established that astrocytes are sensitive to surrounding neuronal activity; in fact, they have receptors for many neurotransmitters including glutamate, GABA, acetylcholine, and ATP (see previously published reviews[2,3,4]). In return, astrocytic processes ensheath synaptic elements and influence neuronal activity both there and at extrasynaptic sites by regulating extracellular ionic homeostasis and releasing several factors or transmitters such as glutamate, D-serine, and ATP[5-7].

The idea that astrocytes can also modulate neuronal function at the network level has emerged, with evidence that astrocytic coupling is spatially regulated and corresponds to neuronal segmentation in areas characterized by a clear anatomical compartmentalization (like areas with sensory representations), indicating that astrocytes will couple to other astrocytes serving the same function rather than just those that are close by. In the lateral superior olive, for instance, most astrocytic networks are oriented orthogonally to the tonotopic axis[8], whereas in the barrel cortex or olfactoty glomeruli, communication between astrocytes is much stronger within barrels or glomeruli and weaker between adjacent ones[9,10]. In both cases, the astrocytic networks are oriented towards the center of the glomerule or barrel[9,10].

We recently showed that astrocytic activity modulates neuronal firing by decreasing the concentration of extracellular Ca^{2+} ($[Ca^{2+}]_e$), presumably through the release of S100β, a Ca^{2+}-binding protein[11]. This effect, which was demonstrated in a population of trigeminal rhythmogenic neurons in the dorsal part of the trigeminal main sensory nucleus (NVsnpr, thought to play an important role in the generation of masticatory movements), results from the fact that rhythmic firing in these neurons depends on a persistent Na^+ current that is promoted by decreases of $[Ca^{2+}]_e$[11,12]. Rhythmic firing in these neurons can be elicited "physiologically" by stimulation of their inputs or artificial decrease of $[Ca^{2+}]_e$. We further showed that astrocytic coupling was required for neuronal rhythmic firing[1]. This raised the possibility that astrocytic networks may form circumscribed functional domains where neuronal activity can be synchronized and coordinated. To assess this hypothesis, we first needed to develop a method to rigorously document the organization of these networks within NVsnpr.

Previous studies on astrocytic networks have mostly described the extent of coupling in terms of

cell number and the density and area covered. Attempts to evaluate the shape of astrocytic networks and the direction of dye-coupling were mostly performed by comparing the size of networks along two axes (x and y) in the barrel cortex[9], hippocampus[13-15], barreloid fields of the thalamus[16], lateral superior olive[8], olfactory glomeruli[10], and cortex[14]. The methods described here enable unbiased counts of labeled cells in a network and an estimation of the area they cover. We also developed tools to define the preferred orientation of coupling within a network and to assess whether the preferred orientation is towards the center of the nucleus or in a different direction. In comparison to previously used methods, this protocol provides a means to describe the organization and orientation of astrocytic networks in structures like the dorsal trigeminal main sensory nucleus that do not have a known anatomical compartmentalization. In the above studies, the network orientation is described as a relationship to the shape of the structure itself which is already documented (*e.g.*, the barreloid in the thalamus, barrels in the cortex, layers in the hippocampus and cortex, glomeruli in the olfactory bulb, etc.). In addition, vectorial analysis allows for comparisons of coupling orientations revealed under different conditions. To analyze whether these parameters changed according to the position of the network within the nucleus, we also developed a method to replace each network in reference to the boundaries of the nucleus. These tools can be easily adapted to other areas for investigating networks of coupled cells.

PROTOCOL:

All procedures abide by the Canadian Institutes of Health Research rules and were approved by the University of Montreal Animal Care and Use Committee.

1. Preparation of Rat Brain Slices

1.1 Prepare 1 L of a sucrose-based solution (**Table 1**) and 1 L of standard artificial cerebral-spinal fluid (aCSF) (**Table 2**).

1.2 Bubble the sucrose-based solution with a mix of 95% O_2 and 5% CO_2 (carbogen) for 30 min before placing it in -80 °C for about 30 min, until the solution is cold but not entirely frozen. Use this ice-cold sucrose as the cutting buffer for the slicing of the brain. Keep it on ice once it is removed from the freezer.

1.3 Bubble the aCSF with carbogen through the entire experiment. Use this solution for slice storage and as the perfusing buffer in which the patch-clamping and biocytin-filling of astrocytes will be performed. Prepare a slice recovery holding chamber to deposit the brain slices as soon as they are cut.

Note: The slice recovery holding chamber could be custom-made and consists essentially of one small well with a mesh at the bottom suspended in a larger well that is filled with aCSF, in which a tube is inserted to bring carbogen from the bottom.

1.4 Use 15- to 21-day-old Sprague-Dawley rats without any sex- or strain-specific bias. Anesthetize the animal with isoflurane (1 mL of isoflurane in an anesthesia induction chamber).

Check the depth of anesthesia by gently pinching the hind paw or tail of the animal.

1.5 Decapitate the rat using a guillotine, cut its skull with scissors, and quickly remove the brain from the cranium with a flat spatula.

1.6 Dip the brain in the ice-cold sucrose-based solution for about 30 s and transfer it (with the solution) to a petri dish. With a razor blade, remove the portions that are anterior and posterior to the area to be sectioned, if cutting slices in the transverse plane.

1.7 Glue the remaining block of brain tissue on its rostral side and proceed to cut brain slices (350 µm thick) in the sucrose-based medium using a vibratome. Then, transfer the collected slices in a recovery holding chamber filled with carbogenated aCSF at room temperature (RT) until they are ready to be used (allow at least 1 hour for recovery).

Note: Recent developments in the field allow prolonged incubation up to 24 h of brain slices in *in vitro* conditions[17].

2. Sulforhodamine 101 (SR-101) Labeling of Astrocytes

2.1 Pre-heat a water bath to 34 °C and place two slice incubation chambers in it. Fill one of the slice incubation chambers with a solution of aCSF containing 1 µM SR-101, and fill the other only with aCSF.

2.2 Incubate the slices in the incubation chamber containing the 1 µM SR-101 for 20 min and then transfer them into the second incubation chamber to rinse out excess SR-101 from the tissue. Let it incubate for 20 min or more at 34 °C, then keep the incubation chamber containing the slices at RT until they are needed[18].

3. Astrocyte Patching and Biocytin Filling

3.1 Select a slice and place it in the recording chamber of the microscope. To patch astrocytes, use electrodes with a resistance of 4-6MΩ when filled with a potassium-gluconate-based solution (see **Table 3**).

3.2 Under visual guidance and using a micromanipulator, direct the recording electrode towards an SR-101-labeled astrocyte as shown in **Figure 1**. Avoid cells located at the surface of the slice since they are more likely to be damaged or have lost connections to neighboring cells.

3.3 To prevent leakage of biocytin in the tissue, minimize the positive pressure added to the patch pipette and apply it only when it is close to the astrocyte that will be patched (0.1-0.4 mL in a syringe of 1 mL).

3.4 Prior to patching, adjust the offset of the pipette and its capacitance. Correct for liquid junction potentials, as accurate and precise voltage commands are critical to the experiments[19].

3.5 Move the pipette close enough to the astrocyte to observe depression caused by the positive pressure. Then, remove the positive pressure and slowly apply some negative pressure. Clamp the astrocyte to -70 mV when the seal reaches 100 MΩ. Wait until the seal reaches 1-3 GΩ. Continue to apply negative pressure until breaking into the cell. Be careful while applying negative pressure, since astrocytes are very fragile.

3.6 Assess the electrophysiological properties of the patched cell. In voltage-clamp mode, perform a whole-cell current-voltage protocol with a ramp voltage command of 600 ms duration ranging from -120 to +110 mV. In current-clamp mode, perform a step IV protocol in which the injection of 1000 ms current steps of 100 pA from -1 to 1 nA, the sampling rate of the whole-cell recordings is 10 kHz.

Note: Astrocytes show a linear current-voltage profile without any kind of rectification (as shown in **Figure 1B**) and no action potential firing upon membrane depolarization (**Figure 1C**). The resting membrane potential (RMP) should be stable and not positive to -60mV. In some brain areas, the RMP of astrocytes is more hyperpolarized than in the NVsnpr.

3.7 Allow the biocytin to diffuse within the astrocyte for 30 min while performing a step IV protocol every 5 min.

3.8 Retract and detach the patch pipette carefully without damaging the patched astrocyte and immediately take note of the offset of the pipette before taking it out of the recording chamber. Subtract that value from the membrane potential recordings.

3.9 Leave the brain slice to rest in the recording chamber for a minimum of 15 min (in addition to the 30 min for injection) to allow spreading of the tracer from the patched astrocyte to the entire network of coupled cells.

Note: To reveal a network of coupled cells, only a single cell should be patched in the nucleus of interest. If multiple attempts are required in order to achieve a successful patch, discard the case and try to patch on the contralateral side or in another brain slice.

3.10 Make a mark or incision in the tissue to identify which side of the slice is facing upwards, and transfer the slice first to a petri dish containing normal aCSF, then into a solution of 4% paraformaldehyde (PFA). Incubate the slice at 4 °C overnight.

CAUTION: PFA is extremely harmful. Use protective equipment in a ventilated hood. Ensure that all materials (brushes, tubes, etc.) that have been in contact with PFA do not contact the recovery holding chamber, incubation chamber, or other materials used for recording the fresh tissue.

4. Biocytin Revelation

4.1 Revelation with fluorescent streptavidine

4.1.1 Wash the brain slices 2 x 10 min in 0.1 M phosphate buffer saline (PBS) at RT. Then, reveal the biocytin by incubating the brain slices with streptavidine conjugated to a fluorophore at 1/200 dilution in PBS with 4% non-ionic detergent for 4 h at RT.

4.1.2 Wash the brain slices 3 x 10 min in 0.1 M PBS at RT and mount the sections on glass slides using an aqueous mounting medium. Face the sides that were injected upwards, coverslip the slides, and seal them with nail-varnish.

4.2 Revelation with DAB

Note: DAB (3,3-diaminobenzidine) revelation can be used when fluorescence cannot be used. In this case, only one revelation method should be employed for making comparisons.

4.2.1 Wash the brain slices 3 x 10 min in PBS at RT. Incubate the slices in PBS + H_2O_2 0.5% for 1 hour at RT.

4.2.2 Rinse the slices 3 x 10 min in PBS at RT. Then, incubate the slices in an avidin-biotin complex staining solution composed of PBS and 1% non-ionic detergent + avidin-biotin complex peroxidase standard staining kit reagents at 1/100 for 24 hours at RT.

4.2.3 Rinse the slices 3 x 10 min in PBS at RT, incubate them in a solution of PBS + DAB 0.05% for 20 min at RT, and transfer them into a solution of PBS + DAB 0.05% + H_2O_2 0.5%.

CAUTION: DAB is extremely harmful. Use protective equipment in a ventilated hood. The color reaction is stopped when the slices are transferred to the PBS.

4.2.4 Rinse the slices 5 x 10 min in PBS at RT, mount the sections on glass slides (face the sides that were injected upwards) and let them dry on a slide drying bench overnight at 34 °C.

4.2.5 Submerge the glass slides for 1 min in several alcohol baths at 70%, 95%, and 100%, and end with a bath of xylene for 1 min.

4.2.6 Mount the glass slides using a toluene-based synthetic resin mounting medium. Place coverslips on the slides and seal them with nail varnish.

5. Network Imaging

5.1 Visualize the astrocytic networks using a scanning confocal microscope equipped with 20X and 4X objectives (or an appropriate objective to visualize the entire nucleus where the network is located) and a laser to detect the fluorophore (in this case, Alexa-594 is used).

5.2 Use the 20X magnification to make a z-stack of the network of labeled cells. Use a resolution of 800 x 800 pixels and scan speed of 12.5 µs/pixel.

Note: In order to image the whole network, multiple stacks are usually required, and the number of stacks needs to be adjusted for each network. The resolution and scan speed can be changed, but make sure to use the same settings to image all data.

5.3 Use the 4X magnification to take images of the network and region of interest.

Note: The 4X imaging is used to determine the network position within the nucleus of interest. Always image the same field in transmitted light. This image will be useful if you cannot determine the border of the nucleus in the confocal fluorescent image.

6. Image Analysis

6.1 Data preparation

6.1.1 Use the software ImageJFIJIFIJI (download it at https://fiji.sc/). Open the file and click OK in the "Bio-Formats Import Options" window.

6.1.2 To redefine a z-stack that will contain only the optical slices needed for the final z-stack (**Figure 2A**), click on the "Stack" knob in the toolbar (to find, first select stk | Z Project). Select "Max Intensity" in the projection type setting (**Figure 2A**). Save the file and name it "stack file".

6.1.3 If the imaging file contains several channels, split it to conserve only the channel with the astrocytic network imaging (Image | Color | Split Channels).

6.1.4 Check the pixel settings of the image [Image | Properties | Pixel (with "1" for pixel dimension)].

6.1.5 Use the subtract background tool (Process | Subtract Background) to remove the background of biocytin labelling. Use the preview function to set the rolling ball radius, which is generally set at 50 pixels (**Figure 2B**).

6.1.6 Use the remove outliers tool (Process | Noise | Remove Outliers) if it is required following the subtract background step. Select "Bright" in the "Which Outliers" setting (**Figure 2C**). Use the preview function to set the radius and threshold. Be careful with this tool, since it may blur the data, as shown in **Figure 2D**.

Note: This tool removes the small spots caused by unspecific deposits of streptavidine (as shown by the white arrows in **Figures 2B** and **2C** before and after treatment, respectively).

6.1.7 Adjust the threshold (Image | Adjust | Threshold). Select "Default" and "B&W" mode (**Figure 2E**). Click on "Apply".

Note: Auto-adjusting can be used, but manual adjusting with the two slider bars is preferred. The

aim of this step is to reduce noise to the maximum without losing any labeled cells.

6.1.8 Convert the image into a binary image with the binary process tool (Process | Binary | Make Binary) as shown in **Figure 2F**. Save the file as a TIFF file and name it "binary file".

6.2 Cell counting

6.2.1 Check the setting of the measure function (Analyze | Set measurement). Select the "Centroid" option.

6.2.2 Use the "Analyze Particles" tool on the "binary file" (**Figure 3A**) produced in the previous step (Analyze | Analyze Particle) (**Figure 3C** on the left). Select "Outlines" in the "Show" setting (**Figure 3C**). This generates a new file that shows the result of the detection (**Figure 3B**).

6.2.3 Play with the parameters: size (to detect only cells, use values between 30 and 6000) and circularity (to determine an interval between 0 to 1, in which "1" defines a perfect circle and "0" a random shape) to refine the detection (**Figure 3C**, left portion). Run the detection by clicking "OK".

Note: Two tables will appear following the detection: 1) a table titled "Summary" that provides the number of detected cells, and 2) a table titled "Results" (**Figure 3C**, right portion) that provides the x- and y-coordinates of each cell.

6.2.4 Copy the values and paste them into a spreadsheet application. Save this table under the name "detection table". A file with a plot of detected cells will also appear (**Figure 3B**). Save this file as a TIFF file under the name "detection file".

6.2.5 If a group of 2 or more labeled cells in the network are detected as a single cell with the analyze particles tool because they are too close to each other, use the watershed tool (Process | Binary | Watershed) **on the binary image** before applying the analyze particles tool, and redo the analyze particles steps.

Note: The watershed tool creates a delimitation of 1 pixel wide between extremely close cells. A cell counter plug-in can be used when labeling is unequivocal and can be conducted manually.

6.3 Measuring astrocytic network area

6.3.1 To measure the surface area of the networks, use the detection file using Image J.

6.3.2 Use the polygon selection tool (left click on the button in the tool bar to select it) to trace a polygon that connects all the cells located in the external periphery of the network (**Figure 4A**). Left click to begin tracing the polygon, and right click to close it.

Note: This polygon will be defined as a region of interest (ROI) and its surface will be measured

to determine the surface area of the network.

6.3.3 Open the set measurement window (Analyze | Set Measurement) and select the “Area” option. Open the ROI Manager (Analyze | Tools | ROI Manager) (**Figure 4B**). Then, add the traced polygon in the ROI Manager by clicking ‘’Add’’ (**Figure 4B**) and run the measurement by clicking ‘’Measure’’ in the ROI Manager.

Note: The area measurement will appear in a table and be expressed in pixels. Do not forget to convert this value with the conversion factor for the microscope used to obtain a value in μm^2.

6.4 Determination of the main direction vector

6.4.1 Determination of the patched cell

6.4.1.1 Open the stack file in ImageJFIJI and identify the patched cell in the stack file based on its stronger labeling intensity (**Figure 4C**). Then, open the file named “detection table” in a spreadsheet application and find the number associated to the patched cell and its corresponding coordinates.

6.4.1.2 If unable to accurately determine the patched cell, surround the area where the deposit of biocytin is denser in the imaged network of coupled cells, using the Polygon tool in ImageJFIJI, and refer to this position as that of the patched cell (**Figure 4D**).

6.4.1.3 Use the ROI Manager (Analyze | Tools | ROI Manager). Then, draw a ROI at the patched cell location and add it to the ROI Manager (see **Figure 4B**).

6.4.1.4 Set a measurement (Analyze | Set Measurement) and select the “Centroid” option.

6.4.1.5 In the ROI Manager, click on “Measure” to obtain the coordinates of the centroid of the traced area. Use these coordinates as the reference point for this specific network.

6.4.2 Referential translation

6.4.2.1 Calculate the coordinates of each cell in reference to the patched astrocyte by using the following formula:

$$(x', y') = (x - x_0, y - y_0)$$

With: (x, y) as the coordinates for a given cell; (x_0, y_0) as the coordinates of the patched cell (or the referential point of the network); and (x', y') as the coordinates for a given cell in the new referential.

Note: Expressing the coordinates of each cell in reference to the patched astrocyte is an important step in calculating vectors from the patched astrocyte. Be careful when using ImageJFIJI that the referential for any image is located in the top-left corner of the image.

6.4.3 Determination of the main vector of preferential orientation

6.4.3.1 Calculate the coordinates of the main vector of preferential orientation with the following formula:

$$(x_p, y_p) = (x'_1 + x'_2 + x'_3 + \cdots, y'_1 + y'_2 + y'_3 + \cdots)$$

With: $(x_p y_p)$ as the coordinates of the main vector of preferential orientation; and $(x'_1, y'_1), (x'_2, y'_2), \ldots$ as the coordinates of each cell of the network obtained with the patched cell as referential.

Note: For each cell in the network, a vector is determined relative to the coordinates of the patched astrocyte. The main vector of preferential orientation of the network is the sum of all these vectors.

6.4.3.2 Divide the length of the main vector (provided by the coordinates obtained from using the above formula) by the number of cells in the network minus one (since the coordinates of the patched cell are not included), to normalize the values and enable comparisons between networks. A schematic view of this analysis is presented in **Figure 5**.

6.5 Placement of analyzed networks in the nucleus of interest

6.5.1 Alignment of the 20X and 4X images

6.5.1.1 To determine the position of each network in the nucleus of interest (NVsnpr), use the 4X image. Open the 4X image with a vector image editor.

6.5.1.2 Select the 4X image and modify its size by multiplying it by 5. The dimension window is located in the right part of the top horizontal toolbar. For instance, for a 4X image that has been sampled at 800 x 800 pixels, change the sampling resolution to 4000 x 4000 pixels (to set the working unit in pixels, go to “Document Setup” under the file tab: File | Document Setup). Export the file in TIFF format and name it “resized 4X”.

6.5.1.3 Align the top-left corner of the image with the bottom-left corner of the Adobe Illustrator document.

Note: The software provides coordinates from a bottom-left corner referential point.

6.5.1.4 Open the 20X image of the network. Use the ‘’binary file’’ or ‘’detection file’’ because they are easier to align. Then, play with the opacity tool on the ‘’binary file’’ of the 20X image to align it with the re-sized 4X image.

Note: The opacity tool is in the top horizontal tool bar.

6.5.1.5 When the alignment is done, select and hold the pipette tool so the measure tool appears, and select it in the left toolbar.

6.5.1.6 Use the measure tool to click on the top-left corner of the 20X image to get the coordinates of the 20X referential point onto the resized 4X image.

Note: These coordinates, which are referred to as the 20X referential (20XR in **Figure 5**), will be useful for expressing the position of each network on a schematic drawing of the nucleus.

6.1.2 Normalization of the nucleus of interest

Note: To sum up the data, a normalization of the nucleus (NVsnpr) as a rectangle is used. The steps are described below.

6.5.2.1 Open the 4X resized file in ImageJFIJI, and use the polygon tool to surround the nucleus (NVsnpr). Use the image with transmitted light if the borders of the nucleus are not able to be seen; in which case, remember to resize it first.

6.5.2.2 Open the ROI Manager and add the drawn ROI. In "Set Measurement", select the ''Bounding Rectangle'' option.

Note: The "Bounding Rectangle" option calculates the smallest rectangle within the drawn nucleus.

6.5.2.3 Click "Measure".

Note: A table appears with BX and BY, the coordinates of the top left corner of the rectangle: ''Rectangle Position'' and provides the width and height. BX and BY are the coordinates of the bounding rectangle referential which are referred to as x_{BR} and y_{BR}.

6.5.3 Expression of each network position in the normalized nucleus

6.5.3.1 Express the coordinates of each cell with the 4X referential (black square in **Figure 5**) using the following formula:

$$(x_{4X}, y_{4X}) = (x_{20X} + x_{20XR}, y_{20X} + y_{20XR})$$

Where: (x_{4X}, y_{4X}) are the cell coordinates with the 4X referential; (x_{20X}, y_{20X}) are the cell coordinates with the 20X referential (orange square in **Figure 5**); and (x_{20XR}, y_{20XR}) are the coordinates of the 20X referential point in the 4X image (20XR).

6.5.3.2 Express the cell coordinates in the bounding rectangle referential (blue in **Figure 5**) using the following formula:

$$(x_R, y_R) = (x_{4X} - x_{BR}, y_{4X} - y_{BR})$$

Where: (x_R, y_R) are the cell coordinates in the bounding rectangle referential; (x_{4X}, y_{4X}) are the cell coordinates in the 4X referential; and (x_{BR}, y_{BR}) are the coordinates of the bounding rectangle referential in the 4X image.

6.5.3.3 Transform the cell coordinates in the bounding rectangle referential to the percentage of width and height of the bounding rectangle using the following formula:

$$(x_{\%}, y_{\%}) = (\frac{x_R}{w} \times 100, \frac{y_R}{h} \times 100\ )$$

Where: $(x_{\%}, y_{\%})$ are the cell coordinates in the percentage of width and height of the bounding rectangle; (x_R, y_R) are the cell coordinates in the bounding rectangle referential; w is the width of the bounding rectangle measured above in the protocol; and h is the height of the bounding rectangle measured above in the protocol.

6.5.3.4 To represent all the networks on the same figure, take into account the orientation of the slice (left or right side). To standardize the data, the referential is applied on the left side of the slice. Transfer the network coordinates of the right side to the left side by applying the following formula only to x-coordinates:

$$x_L = 100 - x_R$$

Where: x_R is the x-coordinate on the right side of the slice; and x_L x$_L$ is the new x-coordinate expressed in the referential on the left side of the slice.

Note: Alternatively, mirror the picture in ImageJFIJI before the analysis (Image | Transform | Flip Horizontally).

6.5.3.5 To express the coordinates of the main vector of preferential orientation, follow the same steps with the cell coordinates (steps 6.5.3.1 to 6.5.3.4).

Note: The expression of the coordinates in percentages allows a compilation of the data as a single plot in which the nucleus (NVsnpr) is designed as a rectangle.

6.6 Study of the angular difference of the main vector of preferential direction

Note: The angular difference of an astrocytic network is used to determine whether its preferential orientation is towards the center of the nucleus of interest. To calculate the angular difference (α in **Figure 5**), which is the angle between the main vector of preferential direction of the network (PD, red line in **Figure 5**) and the line connecting P to C, apply the Al-Kashi Theorem into the triangle PDC (see inset of **Figure 5** and **Supplementary Methods**).

6.6.1 First, calculate the different lengths using the application of the Pythagorean Theorem into a Cartesian referential using the following equation:

$$d = \sqrt{(x_p - x_c)^2 + (y_p - y_c)^2}$$

Where: the coordinates of P and C are (x_p, y_p) and (x_c, y_c), respectively, in the bounding rectangle referential (calculated above).

6.6.2 Determine the angular difference in radians using the following formula:

$$\alpha = \cos^{-1}(d^2 + p^2 - \frac{c^2}{2cd})$$

6.6.3 Convert the angular difference in degrees *(e.g.,* with the DEGREES function in Excel software).

6.6.4 Compile all the angular differences by plotting them in vertical bar charts (**Figures 7C** and **7D**) and determine if there is a preferential orientation of astrocytic networks.

REPRESENTATIVE RESULTS:

Coupling between cells in the brain is not static but rather dynamically regulated by many factors. The methods described were developed to analyze astrocytic networks revealed under different conditions and to understand their organization in NVsnpr. These results have been already published[1]. We performed biocytin filling of single astrocytes in the dorsal part of the NVsnpr in three different conditions: at rest (in control conditions in the absence of any stimulation), in Ca^{2+}-free conditions, and following the electrical stimulation of sensory fibers that project to the nucleus. The experimental settings for the biocytin filling of astrocytes for each condition are illustrated in the left sides of **Figures 6A-C**.

Networks of biocytin-labeled cells were observed in control conditions and confirmed a basal state of cell coupling between NVsnpr astrocytes at rest. In 11 tested cases, biocytin diffusion showed networks composed of 11 ± 3 cells (middle panel in **Figure 6A**, **Figure 6D**) extending over an area of 34737 ± 13254 µm^2 (**Figure 6E**). Carbenoxolone (CBX, 20 µM), a non-specific blocker of gap junctions, was used in an independent set of experiments to ensure that the observed labeling was a result of biocytin diffusion through gap junctions and not uptake by the cells of biocytin, which could leak into the extracellular space from the positive pressure applied to the patch pipette prior to patching. Bath application of CBX reduced the number of labeled cells to 2 ± 0.5 cells (right panel in **Figure 6A**, **Figure 6D**; Iman-Conover method, $P = 0.016$; Holm-Sidak test, $P = 0.010$) and the area of biocytin spread to 2297 ± 1726 µm^2 (**Figure 6E**; Iman-Conover method, $P = 0.0009$; Holm-Sidak test, $P = 0.025$).

The effect of calcium removal from the medium on the NVsnpr astrocytic networks was tested because low extracellular calcium concentration is known to open connexins and gap junctions[20-22], and it can be used as a massive and uniform stimulus to open up the syncytium and maximize tracer diffusion through gap junctions. The astrocytic networks that were revealed in Ca^{2+}-free

conditions (n=10) showed a larger number of cells than the networks revealed in control conditions, with 37 ± 10 labeled cells (middle panel in **Figure 6C, Figure 6D**; Iman-Conover method, $P = 0.016$; Holm-Sidak test, $P < 0.001$) covering an area of 108123 ± 27450 μm^2 (middle panel in **Figure 6C, Figure 6E**; Iman-Conover method, $P = 0.009$; Holm-Sidak test, $P = 0.001$).

Compared to the complete removal of calcium from the medium, electrical stimulation of afferent inputs to the nucleus of interest is a stronger physiological stimulus that directly involves the neuronal circuitry of interest. Consequently, the results from this type of manipulation can provide meaningful information regarding the functional implications of the astrocytic networks observed. For instance, input from two different pathways may lead to different effects on the basal state of cells coupling in a given area, or it may elicit coupling between astrocytes in distinct subdivisions of the nucleus. In our circuit, electrical stimulation of the sensory fibers that project to the NVsnpr using 2-second trains of 0.2 ms pulses at 40-60 Hz (n = 11) produced an increase of the coupling between NVsnpr astrocytes, relative to the unstimulated conditions, with 23 ± 6 cells (middle panel in **Figure 6B**, **Figure 6D**; Iman-Conover method, $P = 0.016$; Holm-Sidak test, $P = 0.012$) spreading out over an area of 814174 ± 15270 μm^2 (middle panel in **Figure 6B**, **Figure 6E**; Iman-Conover method, $P = 0.009$; Holm-Sidak test, $P = 0.004$).

The effects of these two types of stimulation, the removal of calcium from the medium, and the electrical stimulation of afferent inputs, are all disrupted by CBX. The astrocytic networks in this condition comprised only 5 ± 1 cells in Ca^{2+}-free aCSF (right panel in **Figure 6C**, **Figure 6D**; n = 4; Iman-Conover method, $P = 0.016$; Holm-Sidak test, $P < 0.001$) and 9 ± 2 cells with sensory fibers stimulation (right panel in **Figure 6B**, **Figure 6D**; n = 6; Iman-Conover method, $P = 0.016$; Holm-Sidak test, $P = 0.023$). The network surface areas were also reduced to 17987 ± 9843 μm^2 with Ca^{2+}-free aCSF (**Figure 6E**; n = 4; Iman-Conover method, $P = 0.009$; Holm-Sidak test, $P = 0.004$) and to 39379 ± 11014 μm^2 with sensory fibers stimulation (**Figure 6E**; n = 6; Iman-Conover method, $P = 0.009$; Holm-Sidak test, $P = 0.055$).

Anatomical analysis was performed only in cases where the NVsnpr boundaries could be clearly defined on 4X imaging, which was the case for 9 out of 10 networks obtained with Ca^{2+}-free aCSF and 8 out of 11 networks obtained with electrical stimulation. Plotting of all the analyzed astrocytic networks on a theoretical NVnspr shows that most cells comprised in the networks were confined within the nucleus boundaries (**Figures 7A** and **7B**, left and middle panels). Under Ca^{2+}-free aCSF, 4 out of 9 astrocytic networks spread outside of the NVsnpr in the direction of the motor nucleus located medially to the NVsnpr. In these 4 cases, the vast majority of the labeled cells were confined to the nucleus. The networks of labeled cells obtained with electrical stimulation of the sensory fibers were more restricted. Only 2 networks extended over the nucleus borders, in which one spread over the mediodorsal border into the lateral supratrigeminal area (dark green network in **Figure 7B**, left and middle panels). In the second case, 2 astrocytes in the red network (**Figure 7B**, left and middle panels) crossed into the ventral portion of the NVsnpr.

The vectorial analysis for the astrocytic networks preferential orientation (right panel in **Figures 7A** and **7B**) produced different results depending on the stimulus used. Indeed, for the astrocytic

networks observed with Ca^{2+}-free aCSF, all except one of the vectors of preferential orientation were oriented towards the center of the NVsnpr. However, for the astrocytic networks observed with electrical stimulation, the preferential orientation vectors were mostly oriented towards the borders of the nucleus. This is reflected by the computed angular differences in preferential orientation between the astrocytic networks obtained with Ca^{2+}-free aCSF and those obtained with electrical stimulation of the sensory fibers. Under Ca^{2+}-free aCSF, the vertical bar charts of the distribution of angular difference showed that most of the networks of labeled cells have an angular difference between 0 and 40 degrees, with a mean of angular difference of 39.5 ± 12.7 degrees (**Figure 7C**). With electrical stimulation of sensory fibers, the distribution is more uniform, and the mean angular difference (99.5 ± 17 degrees) is significantly different (**Figure 7D**; student t-test, $P = 0.012$).

These data show that biocytin labeling analysis allows us to distinguish the effects of different stimuli modulating astrocytic coupling. Moreover, mapping of the astrocytic networks in a normalized nucleus followed by vectorial analysis provides valuable information on the size and anatomical organization of these networks.

FIGURE AND TABLE LEGENDS:

Figure 1: **Whole-cell patch-clamp of astrocyte.** (A) Astrocytes labeled with a loading of the marker sulforhodamine 101 (SR-101) in NVsnpr. An SR-101-labeled astrocyte soma is targeted with the patch pipette (white dashed line). Scale bar = 100 μm. (B) A depolarizing ramp protocol is performed in voltage-clamp (from -120 to 110mV) to assess the astrocyte passive characteristics. (C) Assessment of the lack of action potential firing in the astrocyte by injection of current pulses in current-clamp mode. This figure is adapted from Condamine *et al.* (2018)[1].

Figure 2: **Treatment and analysis of astrocytic networks with ImageJFIJI software.** (A) Z-Stack creation from the confocal imaging of an astrocytic network. At the top-left, Z-stack window in ImageJFIJI. (B) Background subtraction process. At the top-left, subtract background window in ImageJFIJI. The dotted circle emphasizes the area on the image where the effect of the subtract background command is the more obvious when compared to the image in A. (C) Remove outliers process. This process removes the small spots due to unspecific deposits of streptavidine coupled to an Alexa 594. The white arrows show the deposit prior to (**Figure 2B**) and after (**Figure 2C**) the command has been processed. In the top-left, remove outliers window in ImageJFIJI. (D) Example of the blurring effect that may be produced by an inadequate adjustment of the remove outliers parameters. Yellow arrows show some blurred cells. (E) Adjust threshold process. At the top-left, adjust threshold window in ImageJFIJI. The scroll bars act on the threshold signal adjustment. (F) Make binary step. The image is converted into a binary file in ImageJFIJI. Scale bar = 100 μm.

Figure 3: Detection of cells in astrocytic networks with ImageJFIJ. (A) Example of a binary image of an astrocytic network obtained in ImageJFIJI. Scale bar = 100 μm. (B) Analyze particles window in ImageJFIJI. This function detects the cells of the network in the binary image. The size of the detected cells and their circularity can be adjusted. Numbers to be used should be set by trial-and-error until a satisfactory result is obtained. (C) Illustrates the "detection file" obtained after

applying the analyze particles process on the binary file. The shapes correspond to all the detected cells with their associated number in red. (D) Detection table generated by the analyze particles process. X and Y columns list the coordinates of each cell detected in the image.

Figure 4: Network area analysis and determination of the patched cell in ImageJFIJI. (A) Using the polygon tool in ImageJFIJI, an ROI is traced around the cluster of detected cells (red line) that will be used to determine the surface area of the network. (B) The ROI is added into the ROI Manager. (C) Example of an astrocytic network in which the patched cell (white arrow) is easily identifiable because of the striking intensity of its biocytin labeling. (D) Example of an astrocytic network where the patched cell could not be identified, but where an area of denser labeling clearly indicates biocytin deposits. An ROI is drawn around this area and added to the ROI manager. Its centroid is computed and considered as the position of the patched cell to use for vectorial analysis. Scale bar = 100 μm.

Figure 5: Diagram of the different referentials used for astrocytic networks analysis. The grey square is the 4X image with the referential point 4XR to be aligned with the left bottom corner of the Adobe Illustrator document. The white square surrounded in orange is the 20X image with the referential point 20XR. Both images are aligned with each other as described in the protocol. The bounding rectangle (blue) defines NVsnpr (purple dashed line) and is scaled in percentage with the referential point (BR). The theoric center of the dorsal part of NVsnpr is schematized by the dark blue dot (C). The astrocytic network is schematized by the patched cell (black dot, P) and the main vector of the preferential direction (red line). Each dashed black line is the vector of each cell of the astrocytic network. The angular difference of the astrocytic network (α) is the angle between the main preferential orientation of the network (red line) and the black line that connects the patched astrocyte to the theoretical center of the nucleus. Inset is a zoom of the 20X image showing the triangle PCD formed by the theoretical center of the NVsnpr (C), the patched cell, and the main vector of preferential direction (D).

Figure 6: **Astrocytic networks labeled with biocytin in NVsnpr under different conditions showing different sizes.** (A-C) To the left, a schematic drawing of the experimental condition. In all conditions, a single astrocyte labeled by SR-101 was targeted for whole-cell recording and filled with biocytin (0.2%). Middle column: photomicrographs illustrating the astrocytic networks obtained under control conditions (A), after electrical stimulation of the V^{th} tract (2 s trains, 40-60 Hz, 10-300 μA, 0.2 ms pulses) (B); and after perfusion with a Ca^{2+}-free aCSF (C). Right column: photomicrographs illustrating the astrocytic networks obtained under the same conditions but in the presence of CBX (20 μM) in the bath prior. Scale bar = 100 μm. (D and E) Vertical bars chart representing the number of coupled cells and the surface area, respectively, of the biocytin-filled networks of astrocytes under the three experimental conditions presented above (A, B, and C) in the presence (hatched) and absence (solid) of CBX (20 μM). Data are represented as mean ± SEM. Multiple comparisons (Holm-Sidak test): * = $P < 0.05$; ** = $P < 0.001$. This figure is adapted from Condamine *et al.* (2018)[1].

Figure 7: Characterisation of networks in NVsnpr under Ca^{2+}-free aCSF and with electrical stimulation of the V^{th} tract. (A and B) *Left:* All cells labeled in 9 networks filled under perfusion

with Ca^{2+}-free aCSF (A) or in 8 networks filled while stimulating the V^{th} tract (B) are plotted according to their position in a theoretical NVsnpr nucleus (gray rectangle). Each network (and the cells composing it) is represented by a different color. *Middle*: Boundaries of each network. The dot in each area represents the patched cell. *Right*: Representation of main vector of preferential orientation of each network. The dot represents the patched cell and the arrow the vector of preferential direction. (C and D) Distribution of angular differences between the main vector of the preferential orientation and a straight line connecting the patched cell to the center of the dorsal part of NVsnpr (located at 25% on the dorsoventral axis and 50% on the mediolateral axis) under the two conditions studied. The mean angular difference was 39.5 ± 12.7 degrees in Ca^{2+}-free aCSF, indicating a preferential orientation towards the centre of the nucleus and 99.5 ± 17 degrees with electrical stimulation, indicating a preferential orientation towards the periphery (student t-test, $P = 0.012$). This figure is adapted from Condamine *et al.* (2018)[1].

Table 1: Composition of the sucrose-based solution used for brain slicing. (*) = pH and osmolarity were adjusted to 7.3-7.4 and 300-320 mosmol/kg, respectively.

Table 2: Composition of the aCSf solution used for slice storage and whole-cell recording. (*) = pH and osmolarity were adjusted to 7.3-7.4 and 290-300 mosmol/kg, respectively.

Table 3: Composition of the internal solution used for whole-cell recording. (*) = pH and osmolarity were adjusted to 7.2-7.3 and 280-300 mosmol/kg, respectively.

DISCUSSION:

A number of electrophysiological methods exist to assess functional coupling between astrocytes[23,24]. However, these methods do not provide information about the anatomical arrangement of astrocytic networks. A number of studies have already shown that "dye- or tracer-coupling", as done here, occurs only in a fraction of coupled cells that are detected by electrophysiological methods[25-27], suggesting that the number of cells detected with this method is underestimated. Nevertheless, this is still the best method for visualisation of coupling. Greater dye-coupling is obtained when using molecule tracers smaller than 1-1.2 KDa to permeate gap junctions[20]. Live visualization of coupling can be performed by monitoring diffusion of fluorescent glucose derivatives (2-NBDG) or a fluorescent marker (like some Alexa dyes or Lucifer Yellow)[13], but due to its smaller size, biocytin yields better results and allows for quantification in fixed tissue. Thus, it should be noted that the number of cells detected with this method is largely underestimated. On the other hand, some of the cells may be labeled not because of their coupling, but because of the uptake of tracer that has leaked into the extracellular space. The extent of labeling resulting from leakage can be estimated in control experiments with bath applications of a gap junction blocker[1]. However, it can be assumed that any bias due to the method would apply to all conditions.

Finally, it should be emphasized that not all coupled cells are astrocytes. Panglial networks where astrocytes are coupled to oligodendrocytes have been described in several brain areas, including the lateral superior olive[8], thalamus[16], cortex, and hippocampus[28]. Our aim was to develop a method of comparing astrocytic networks revealed with dye-coupling under different conditions

to assess the hypothesis that they form well-defined, distinctive functional domains revealed by different stimuli. Since in NVsnpr, the trigeminal brainstem nucleus in which this protocol was conducted, coupling between astrocytes is very limited under resting conditions, it was important to first develop a reliable and unbiased method to detect labeled cells. This was achieved with automated detection with ImageJFIJI. It is sometimes difficult to distinguish faintly labeled cells from background noise. Here, stack imaging and a method in ImageJFIJI are used to improve the signal, but background noise can still be too high and lead to data rejection. In future studies, clarification protocols may be used to improve the signal-to-noise ratio. A clearing protocol is an interesting method of clarification that preserves tissue morphology (no shrinkage), does not affect lipids, and is compatible with immunostaining[29]. Another limitation of the method described is the "watershed" tool used to discriminate cells that are too close to each other. Visual inspection of detected cells should be done when using this tool.

If astrocytic networks form functional domains, then they may define the boundaries of a nucleus or should at least be confined to the boundaries of a nucleus. Revealed networks may always be confined within a nucleus, more so if they are smaller in size, if the patched astrocyte is in the center (or within) the nucleus. To test if astrocytes sitting near the border of a nucleus preferably couple with other astrocytes outside the nucleus or with others within the nucleus, we needed to determine the preferential direction to which the dye spread from the patched astrocyte. Several other studies have addressed a similar issue in the barrel cortex, barreloid fields of the thalamus, olfactory glomeruli, hippocampus, and lateral superior olive, but they focused analyses mostly on the distance of diffusion of the tracer, electrophysiological characterization of different types of astrocytes in function of their localization, and spread of dye along orthogonal axes with respect to these well-defined structures[8-10,13,14,16]. Here, we used vectorial analysis to determine the dominant direction of tracer spread, which was given by the size and orientation of the normalized main vector. Small vectors indicate no clear "dominant" or preferential orientation. A critical step for vectorial analysis is the ability to accurately identify the patched astrocyte, which is not always possible. An interesting alternative to help locate the patched astrocyte is to add a large (non-gap junction permeant) and fixable tracer, like dextrans, to the recording solution. If it is not possible to determine the patched cell or patch location, it may be better to omit these experiments from the vector analysis.

Finally, to analyze whether properties of networks varied according to their location in the nucleus, we needed a method to express their position in a "normalized" nucleus. The only critical step in this procedure is the ability to clearly see the borders of the nucleus in the low magnification images (4X). A simple solution to this problem, if it occurs often, is to add a standard histological coloration to tissue processing before analysis.

Heterogeneity of astrocytes across brain regions is clearly established, and a growing body of evidence supports the concept that their specializations are particularly adapted for the function of the circuit that they are embedded in[9,10,30,31]. For this to be true, inter-astrocytic communication should be limited to astrocytes associated to the same circuit. Observations supporting this assumption are emerging in different brain areas but are more evident in areas with clustered representations, like sensory maps in the barrel cortex or olfactory bulb. However,

most reports of overlap between neuronal and astrocytic maps are descriptive and qualitative. The methods reported here can be used to quantify these observations and develop tools to better analyze astrocytic networks according to their position in a given circuit.

ACKNOWLEDGMENTS:

This work is funded by the Canadian Institutes of Health Research, Grant/Award Number: 14392.

DISCLOSURES:

The authors have nothing to disclose.

REFERENCES:

1 Condamine, S., Lavoie, R., Verdier, D., Kolta, A. Functional rhythmogenic domains defined by astrocytic networks in the trigeminal main sensory nucleus. *Glia.* **66** (2), 311-326 (2018).

2 Verkhratsky, A., Orkand, R. K., Kettenmann, H. Glial calcium: homeostasis and signaling function. *Physiological Review.* **78** (1), 99-141 (1998).

3 Christensen, R. K., Petersen, A. V., Perrier, J. F. How do glial cells contribute to motor control? *Current Pharmaceutical Design.* **19** (24), 4385-4399 (2013).

4 Verkhratsky, A., Steinhauser, C. Ion channels in glial cells. *Brain Research Review.* **32** (2-3), 380-412 (2000).

5 Harada, K., Kamiya, T., Tsuboi, T. Gliotransmitter Release from Astrocytes: Functional, Developmental, and Pathological Implications in the Brain. *Frontiers Neuroscience.* **9,** 499 (2015).

6 Montero, T. D., Orellana, J. A. Hemichannels: new pathways for gliotransmitter release. *Neuroscience.* **286,** 45-59 (2015).

7 Araque, A., *et al.* Gliotransmitters travel in time and space. *Neuron.* **81** (4), 728-739 (2014).

8 Augustin, V., *et al.* Functional anisotropic panglial networks in the lateral superior olive. *Glia.* **64** (11), 1892-1911 (2016).

9 Houades, V., Koulakoff, A., Ezan, P., Seif, I., Giaume, C. Gap junction-mediated astrocytic networks in the mouse barrel cortex. *Journal of Neuroscience.* **28** (20), 5207-5217 (2008).

10 Roux, L., Benchenane, K., Rothstein, J. D., Bonvento, G., Giaume, C. Plasticity of astroglial networks in olfactory glomeruli. *Proceedings of the National Academy of Science of the United State of America.* **108** (45), 18442-18446 (2011).

11 Morquette, P., *et al.* An astrocyte-dependent mechanism for neuronal rhythmogenesis. *Nature Neuroscience.* **18** (6), 844-854 (2015).

12 Brocard, F., Verdier, D., Arsenault, I., Lund, J. P., Kolta, A. Emergence of intrinsic bursting in trigeminal sensory neurons parallels the acquisition of mastication in weanling rats. *Journal of Neurophysiology.* **96** (5), 2410-2424 (2006).

13 Anders, S., *et al.* Spatial properties of astrocyte gap junction coupling in the rat hippocampus. *Philosophical Transactions of the Royal Society of London. Series B, Biological Science.* **369** (1654), 20130600 (2014).

14 Houades, V., *et al.* Shapes of astrocyte networks in the juvenile brain. *Neuron Glia Biology.*

2 (1), 3-14 (2006).
15 Rouach, N., Koulakoff, A., Abudara, V., Willecke, K., Giaume, C. Astroglial metabolic networks sustain hippocampal synaptic transmission. *Science.* **322** (5907), 1551-1555 (2008).
16 Claus, L., *et al.* Barreloid Borders and Neuronal Activity Shape Panglial Gap Junction-Coupled Networks in the Mouse Thalamus. *Cerebral Cortex.* **28** (1), 213-222 (2018).
17 Cameron, M. A., *et al.* Prolonged Incubation of Acute Neuronal Tissue for Electrophysiology and Calcium-imaging. *Journal of Visualized Experiments.* (120), (2017).
18 Kafitz, K. W., Meier, S. D., Stephan, J., Rose, C. R. Developmental profile and properties of sulforhodamine 101--Labeled glial cells in acute brain slices of rat hippocampus. *Journal of Neuroscience Methods.* **169** (1), 84-92 (2008).
19 Neher, E. Correction for liquid junction potentials in patch clamp experiments. *Methods in Enzymology.* **207,** 123-131 (1992).
20 Giaume, C., Leybaert, L., Naus, C. C., Saez, J. C. Connexin and pannexin hemichannels in brain glial cells: properties, pharmacology, and roles. *Frontiers in Pharmacology.* **4,** 88, (2013).
21 Torres, A., *et al.* Extracellular Ca(2)(+) acts as a mediator of communication from neurons to glia. *Science Signaling.* **5** (208), ra8 (2012).
22 Ye, Z. C., Wyeth, M. S., Baltan-Tekkok, S., Ransom, B. R. Functional hemichannels in astrocytes: a novel mechanism of glutamate release. *Journal of Neuroscience.* **23** (9), 3588-3596 (2003).
23 Ma, B., *et al.* Gap junction coupling confers isopotentiality on astrocyte syncytium. *Glia.* **64** (2), 214-226 (2016).
24 Meme, W., Vandecasteele, M., Giaume, C., Venance, L. Electrical coupling between hippocampal astrocytes in rat brain slices. *Neuroscience Research.* **63** (4), 236-243 (2009).
25 Ransom, B. R., Kettenmann, H. Electrical coupling, without dye coupling, between mammalian astrocytes and oligodendrocytes in cell culture. *Glia.* **3** (4), 258-266 (1990).
26 Audesirk, G., Audesirk, T., Bowsher, P. Variability and frequent failure of lucifer yellow to pass between two electrically coupled neurons in Lymnaea stagnalis. *Journal of Neurobiology.* **13** (4), 369-375 (1982).
27 Ewadinger, N., Syed, N., Lukowiak, K., Bulloch, A. Differential Tracer Coupling between Pairs of Identified Neurones of the Mollusc Lymnaea Stagnalis. *Journal of Experimental Biology.* **192** (1), 291-297 (1994).
28 Griemsmann, S., *et al.* Characterization of Panglial Gap Junction Networks in the Thalamus, Neocortex, and Hippocampus Reveals a Unique Population of Glial Cells. *Cerebral Cortex.* **25** (10), 3420-3433 (2015).
29 Kuwajima, T., *et al.* ClearT: a detergent- and solvent-free clearing method for neuronal and non-neuronal tissue. *Development.* **140** (6), 1364-1368 (2013).
30 Gourine, A. V., *et al.* Astrocytes control breathing through pH-dependent release of ATP. *Science.* **329** (5991), 571-575 (2010).
31 Forsberg, D., Ringstedt, T., Herlenius, E. Astrocytes release prostaglandin E2 to modify respiratory network activity. *eLife.* **6**, (2017).

Figure 1

Click here to download Figure Figure 1.eps

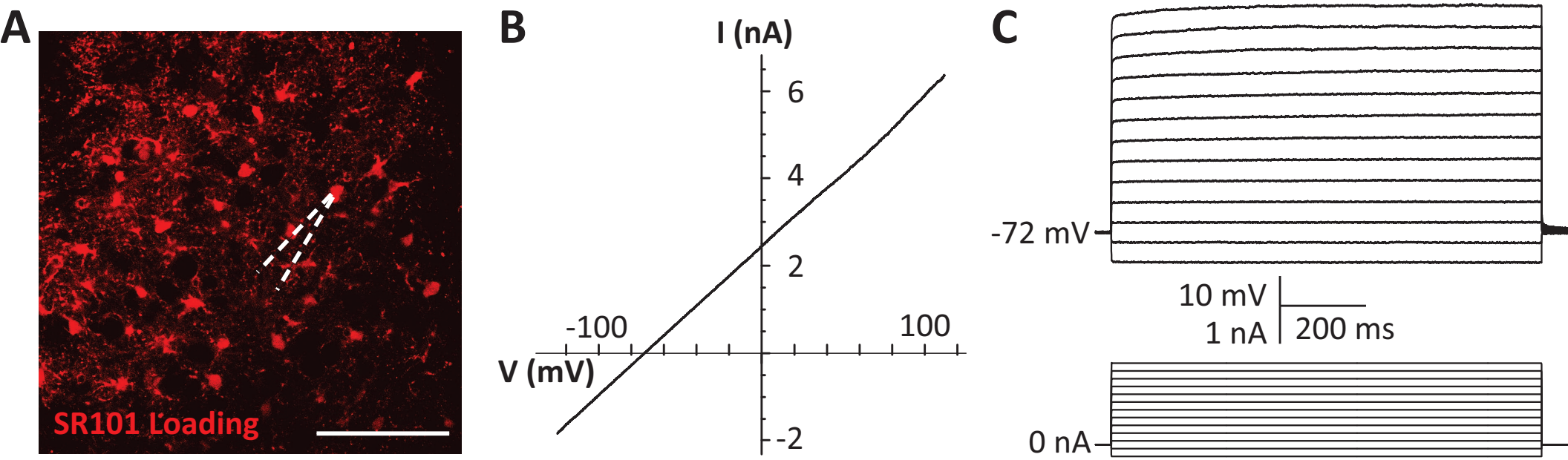

Figure 2

Click here to download Figure Figure 2.eps

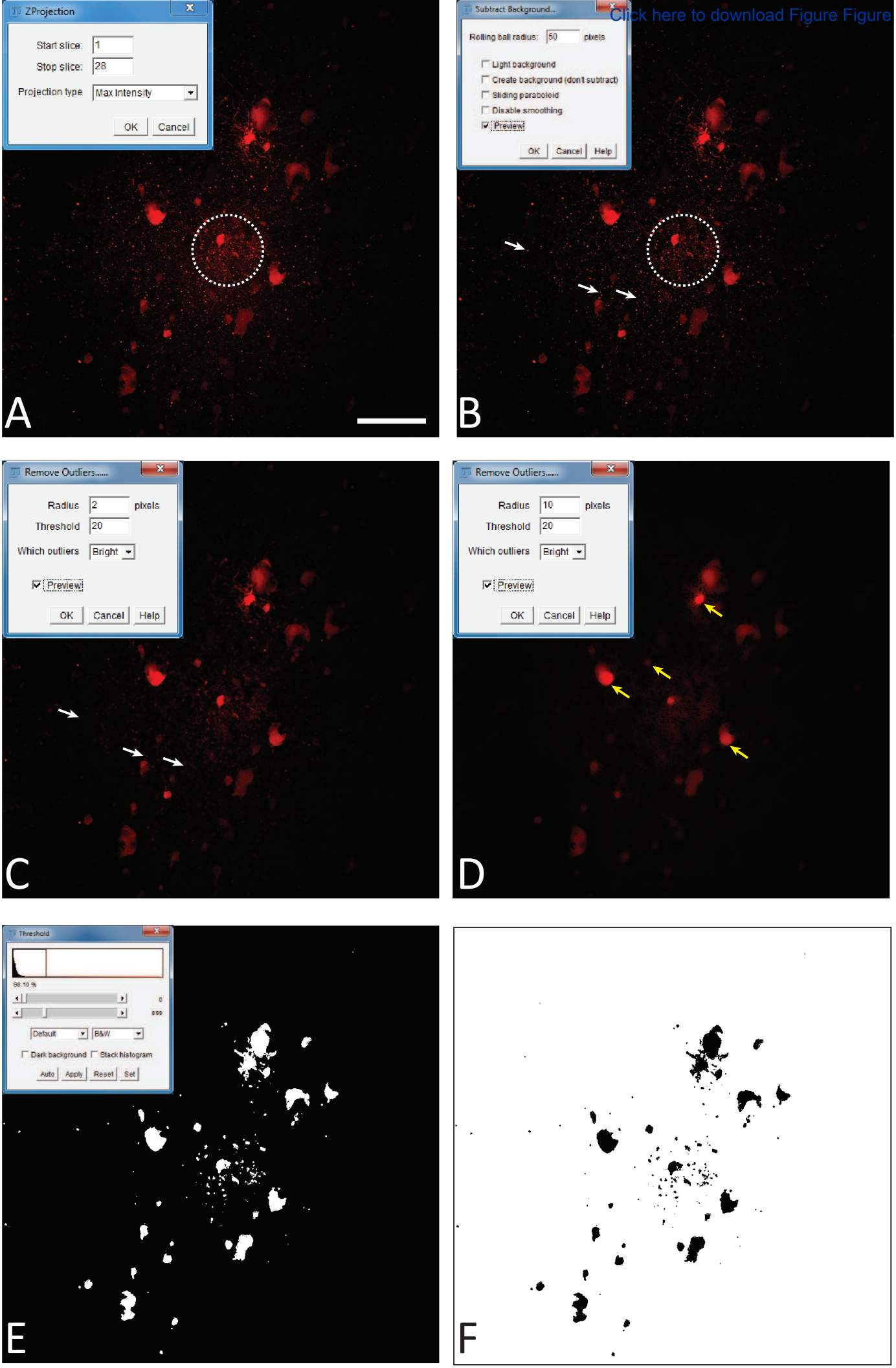

Figure 3

Click here to download Figure Figure 3.eps

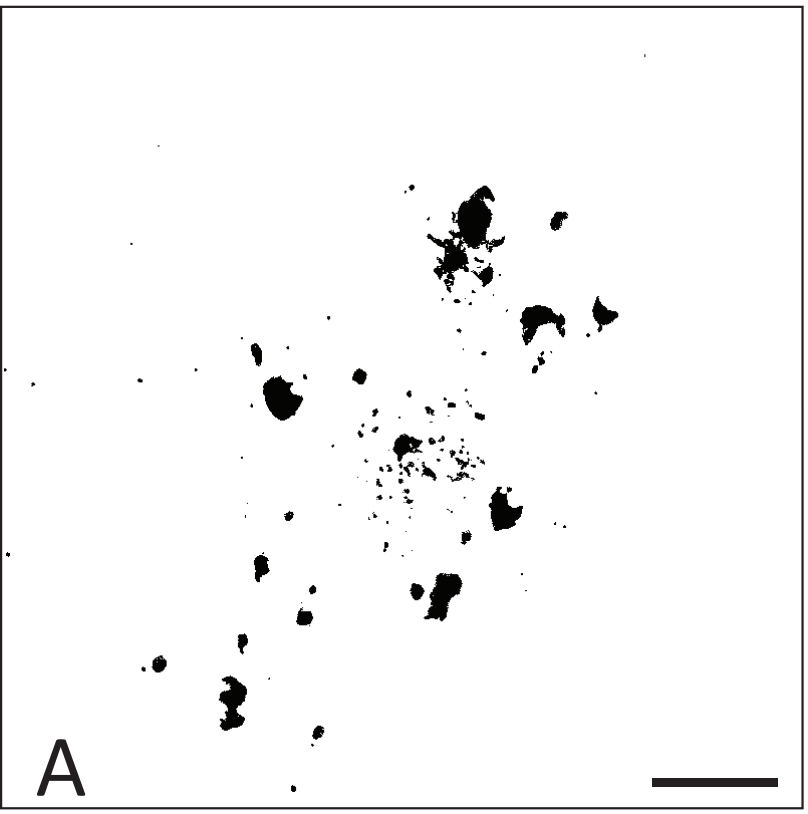

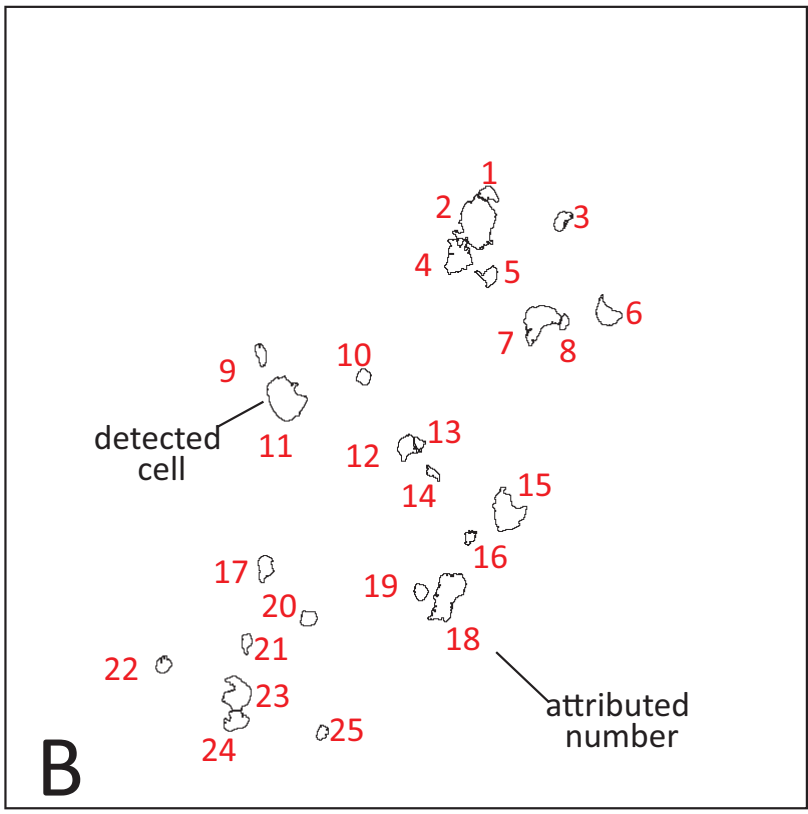

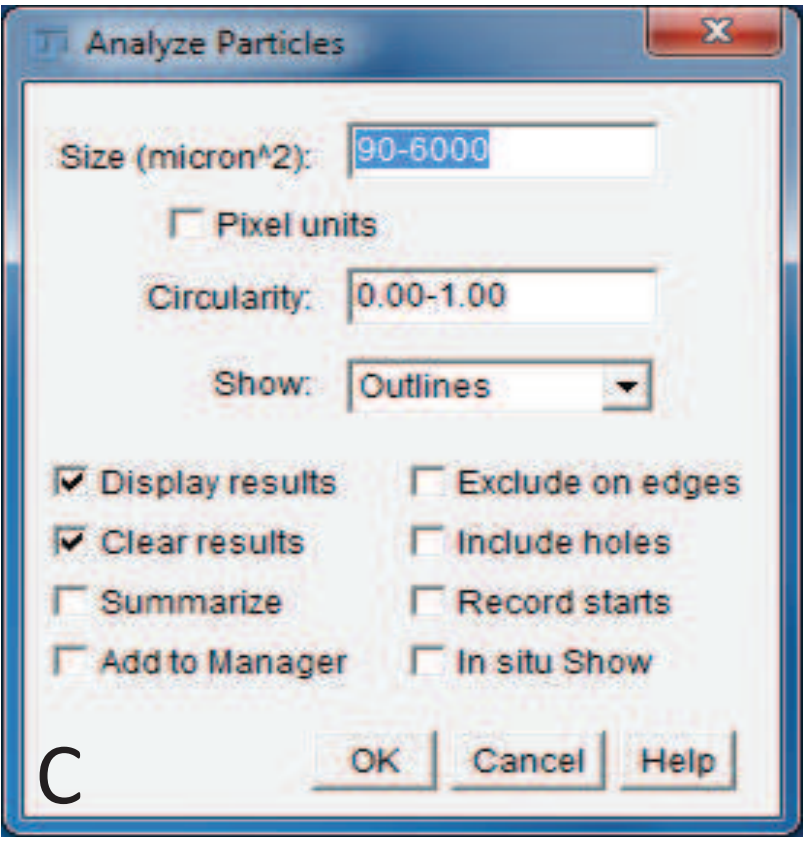

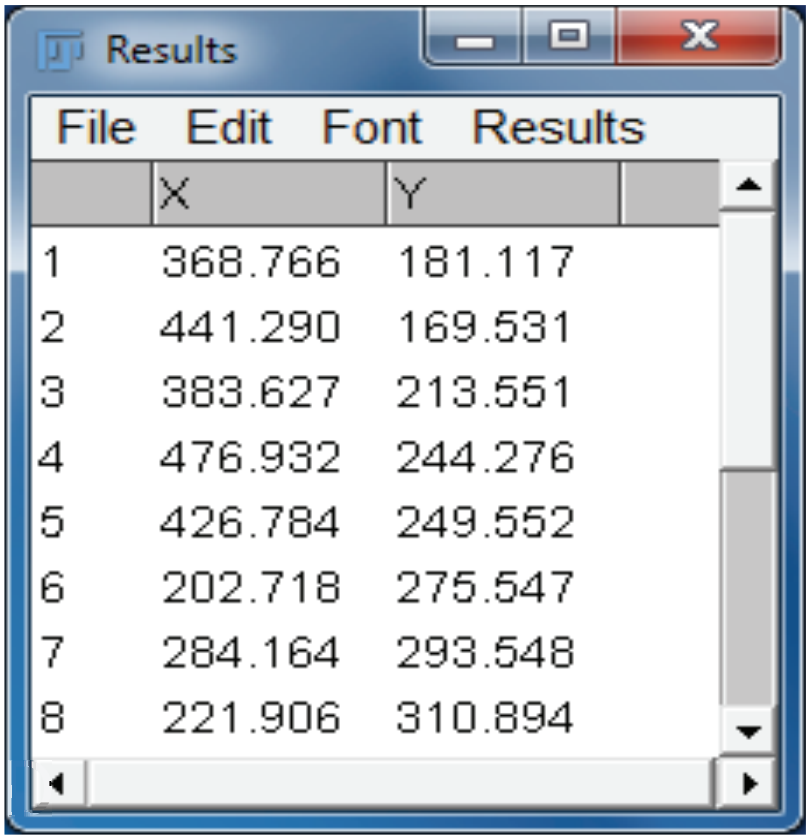

Figure 4

Click here to download Figure Figure 4.eps

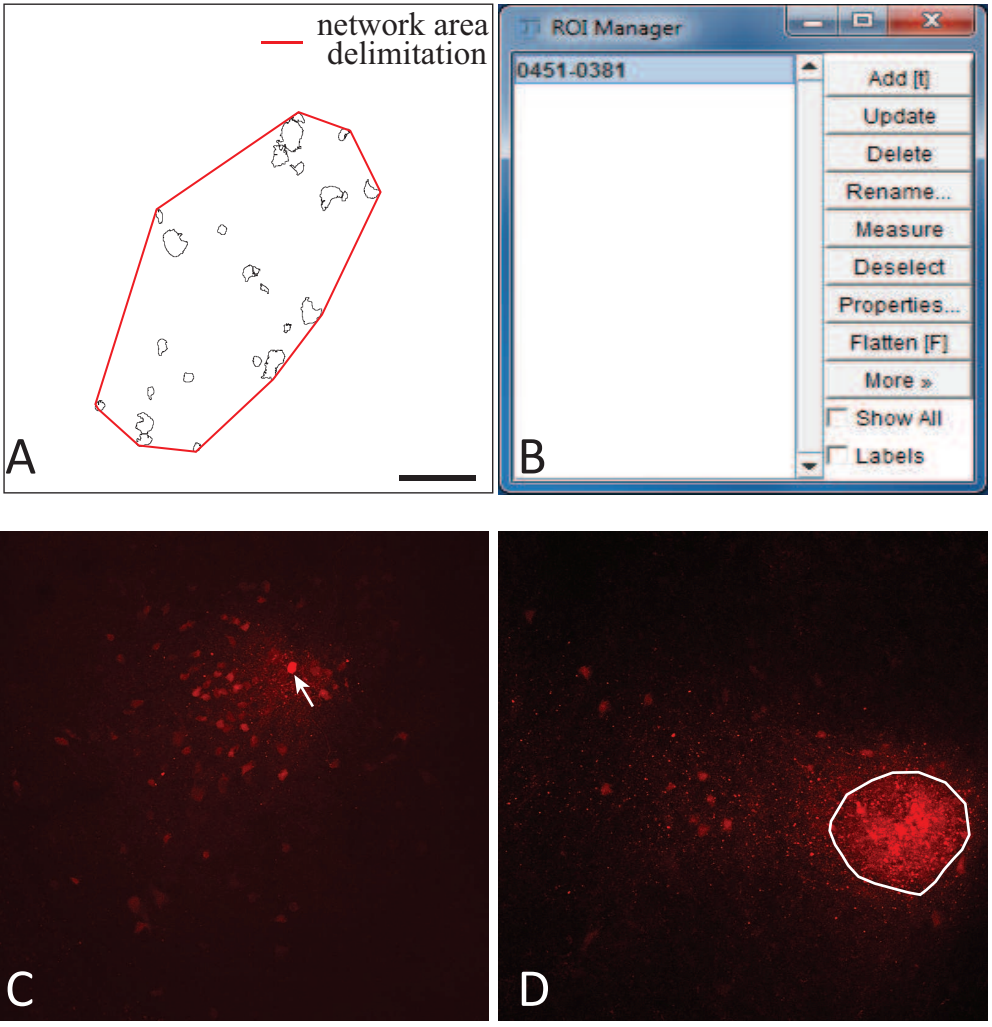

Figure 5

Click here to download Figure Figure 5.eps

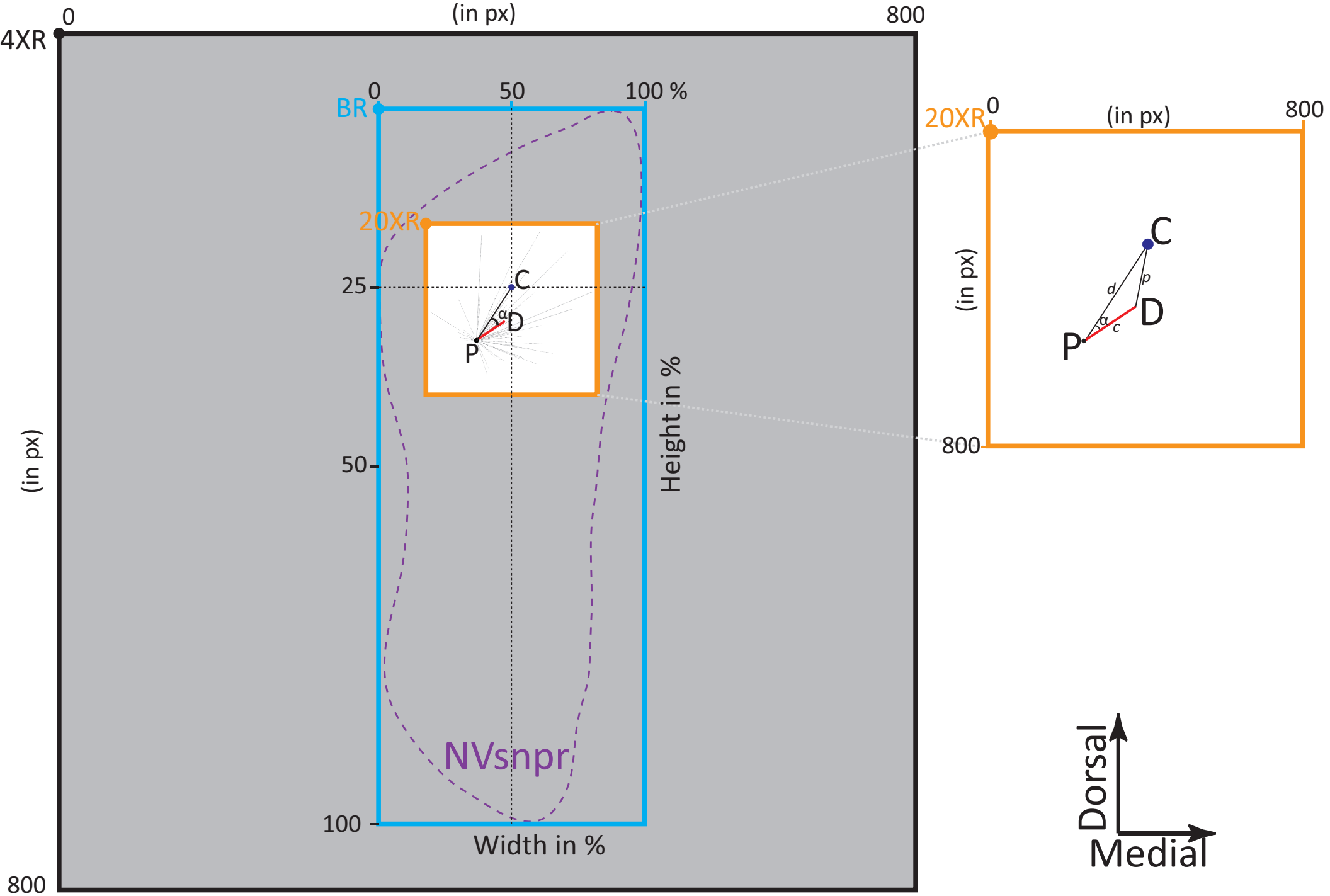

Figure 6

Click here to download Figure figure 6.pdf

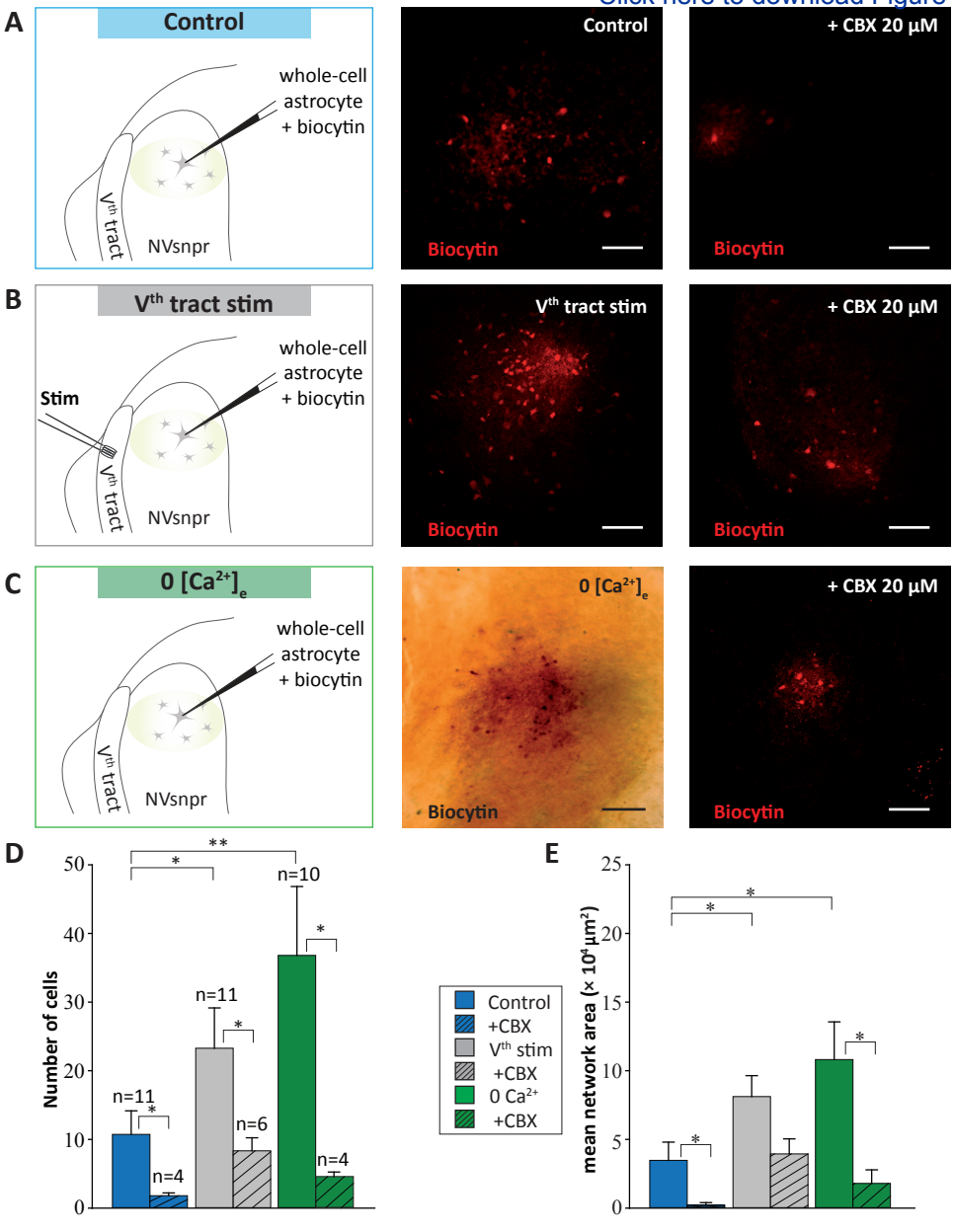

Figure 7

Click here to download Figure figure 7.eps

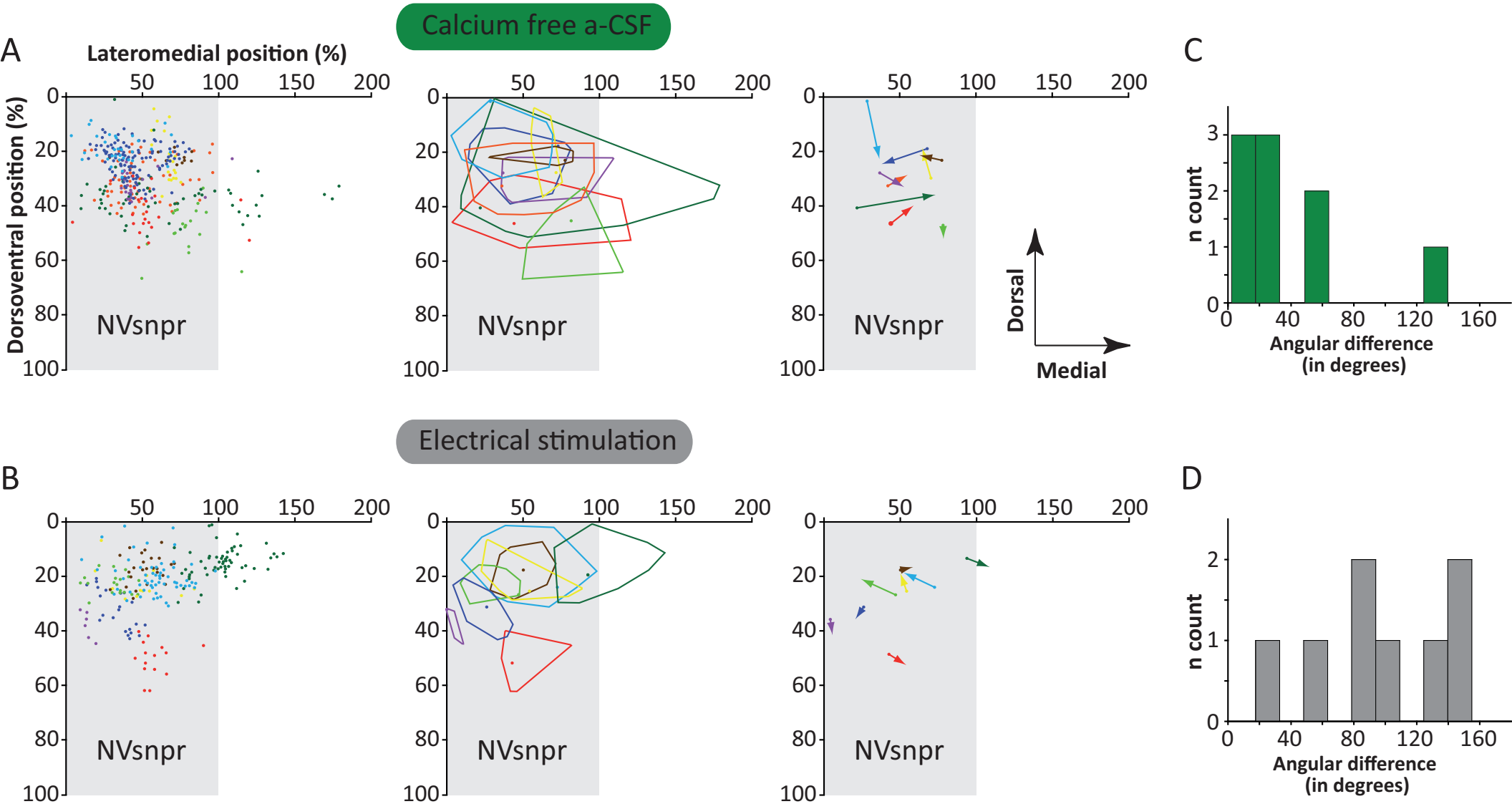

Table 1

Click here to download Table Table 1.xlsx

sucrose-aCSF*	**mMol**
Sucrose	219
KCl	3
KH_2PO_4	1.25
$MgSO_4$	4
$NaHCO_3$	26
Dextrose	10
$CaCl_2$	0.2

Table 2

Click here to download Table Table 2.xlsx

aCSF*	mMol
NaCl	124
KCL	3
KH_2PO_4	1.25
$MgSO_4$	1.3
$NaHCO_3$	26
Dextrose	10
$CaCl_2$	1.6

Table 3

Click here to download Table Table 3.xlsx

Internal patch solution*	mMol
K-gluconate	140
NaCl	5
HEPES	10
EGTA	0.5
Tris ATP salt	2
Tris GTP salt	0.4

Table of Materials

Click here to download Table of Materials JoVE_Materials Revised Condamine Steven.xls

Name of Material/ Equipment	Company	Catalog Number
NaCl	Fisher Chemicals	S671-3
KCl	Fisher Chemicals	P217-500
KH_2PO4	Fisher Chemicals	P285-500
$MgSO_4$	Fisher Chemicals	M65-500
$NaHCO_3$	Fisher Chemicals	S233-500
$C_6H_{12}O_6$ Dextrose anhydrous	Fisher Chemicals	D16-500
$CaCl_2$ dihydrated	Sigma	C70-500
Sucrose	Sigma	S9378
D-gluconic acid potassium salt	Sigma	G45001
$MgCl_2$ anhydrous	Sigma	M8266
HEPES	Sigma	H3375
EGTA	Sigma	E4378
$ATP_{Tris\ Salt}$	Sigma	A9062
$GTP_{Tris\ Salt}$	Sigma	G9002
Biocytin	Sigma	B4261
Carbenoxolone disodium salt	Sigma	C4790
avidin-biotin complex : ABC kit	Vestor laboratories	PK-4000
Streptavidine-alexa 594	Molecular Probes	S11227
Triton	Fisher Chemicals	BP151-500
Xylene	Fisher Chemicals	X5-1
Aqueous mounting medium 1 : Fluoromount-G	SouthernBiotech	0100-01
Toluen-based synthetic resin mounting medium : Permount	Fisher Chemicals	SP15-100
Slide Drying Bench	Fisherbrand	11-474-470
Vibratome	Leica	VT 1000S
Microscope cover glass	Fisherbrand	12-544A
Microscope slide ColorFrost	Fisherbrand	12-550-413
PFA	Fisherchemicals	04042-500

Olympus FluoView FV 1000		
Confocal microscope	Olympus	
40X water-immersion lens	Olympus	LUMPLFLN40XW
20X water-immersion lens	Olympus	XLUMPLFL20XW
4X water-immersion lens	Olympus	XLFLUOR4X/340
Micropipette puller	Sutter Instrument	P97
Micromanipulator	Sutter Instrument	MP 225
Camera CCD	Sony	CX-ST50
Black and white monitor	Sony	SSM-125
Digidata	Molecular devices	1322A
Patch Clamp amplifier	Axon instrument	Mulitclamp 700A
Electrophysiology acquisition software	Molecular devices	pClamp 8
Electrophysiology analysis software	Molecular devices	Clampfit 8
Imaging analysis software	ImageJFIJI	Open source softwa
Vector image editor	Adobe	Illustrator CS4
Spreadsheet application	Microsoft Office	Excel 2010

Comments/Description

are. FIJI version including plug in package.

Author License Agreement (ALA)

Click here to download Author License Agreement (ALA) Author Licence Agreement.pdf

jove JOURNAL OF VISUALIZED EXPERIMENTS

1 Alewife Center #200
Cambridge, MA 02140
tel. 617.945.8051
www.jove.com

ARTICLE AND VIDEO LICENSE AGREEMENT

Title of Article: Methods to analyze size, shape and directionality of networks of coupled astrocytes

Author(s): Steven Condamine, Dorly Verdier, Arlette Kolta

Item 1 (check one box): The Author elects to have the Materials be made available (as described at http://www.jove.com/author) via: ☑ Standard Access ☐ Open Access

Item 2 (check one box):

☑ The Author is NOT a United States government employee.

☐ The Author is a United States government employee and the Materials were prepared in the course of his or her duties as a United States government employee.

☐ The Author is a United States government employee but the Materials were NOT prepared in the course of his or her duties as a United States government employee.

ARTICLE AND VIDEO LICENSE AGREEMENT

1. Defined Terms. As used in this Article and Video License Agreement, the following terms shall have the following meanings: "**Agreement**" means this Article and Video License Agreement; "**Article**" means the article specified on the last page of this Agreement, including any associated materials such as texts, figures, tables, artwork, abstracts, or summaries contained therein; "**Author**" means the author who is a signatory to this Agreement; "**Collective Work**" means a work, such as a periodical issue, anthology or encyclopedia, in which the Materials in their entirety in unmodified form, along with a number of other contributions, constituting separate and independent works in themselves, are assembled into a collective whole; "**CRC License**" means the Creative Commons Attribution-Non Commercial-No Derivs 3.0 Unported Agreement, the terms and conditions of which can be found at: http://creativecommons.org/licenses/by-nc-nd/3.0/legalcode; "**Derivative Work**" means a work based upon the Materials or upon the Materials and other pre-existing works, such as a translation, musical arrangement, dramatization, fictionalization, motion picture version, sound recording, art reproduction, abridgment, condensation, or any other form in which the Materials may be recast, transformed, or adapted; "**Institution**" means the institution, listed on the last page of this Agreement, by which the Author was employed at the time of the creation of the Materials; "**JoVE**" means MyJove Corporation, a Massachusetts corporation and the publisher of *The Journal of Visualized Experiments;* "**Materials**" means the Article and / or the Video; "**Parties**" means the Author and JoVE; "**Video**" means any video(s) made by the Author, alone or in conjunction with any other parties, or by JoVE or its affiliates or agents, individually or in collaboration with the Author or any other parties, incorporating all or any portion of the Article, and in which the Author may or may not appear.

2. Background. The Author, who is the author of the Article, in order to ensure the dissemination and protection of the Article, desires to have the JoVE publish the Article and create and transmit videos based on the Article. In furtherance of such goals, the Parties desire to memorialize in this Agreement the respective rights of each Party in and to the Article and the Video.

3. Grant of Rights in Article. In consideration of JoVE agreeing to publish the Article, the Author hereby grants to JoVE, subject to **Sections 4** and **7** below, the exclusive, royalty-free, perpetual (for the full term of copyright in the Article, including any extensions thereto) license (a) to publish, reproduce, distribute, display and store the Article in all forms, formats and media whether now known or hereafter developed (including without limitation in print, digital and electronic form) throughout the world, (b) to translate the Article into other languages, create adaptations, summaries or extracts of the Article or other Derivative Works (including, without limitation, the Video) or Collective Works based on all or any portion of the Article and exercise all of the rights set forth in (a) above in such translations, adaptations, summaries, extracts, Derivative Works or Collective Works and (c) to license others to do any or all of the above. The foregoing rights may be exercised in all media and formats, whether now known or hereafter devised, and include the right to make such modifications as are technically necessary to exercise the rights in other media and formats. If the "Open Access" box has been checked in **Item 1** above, JoVE and the Author hereby grant to the public all such rights in the Article as provided in, but subject to all limitations and requirements set forth in, the CRC License.

4. Retention of Rights in Article. Notwithstanding the exclusive license granted to JoVE in **Section 3** above, the Author shall, with respect to the Article, retain the non-exclusive right to use all or part of the Article for the non-commercial purpose of giving lectures, presentations or teaching classes, and to post a copy of the Article on the Institution's website or the Author's personal website, in each case provided that a link to the Article on the JoVE website is provided and notice of JoVE's copyright in the Article is included. All non-copyright intellectual property rights in and to the Article, such as patent rights, shall remain with the Author.

5. Grant of Rights in Video – Standard Access. This **Section 5** applies if the "Standard Access" box has been checked in **Item 1** above or if no box has been checked in **Item 1** above. In consideration of JoVE agreeing to produce, display or otherwise assist with the Video, the Author hereby acknowledges and agrees that, Subject to **Section 7** below, JoVE is and shall be the sole and exclusive owner of all rights of any nature, including, without limitation, all copyrights, in and to the Video. To the extent that, by law, the Author is deemed, now or at any time in the future, to have any rights of any nature in or to the Video, the Author hereby disclaims all such rights and transfers all such rights to JoVE.

6. Grant of Rights in Video – Open Access. This **Section 6** applies only if the "Open Access" box has been checked in **Item 1** above. In consideration of JoVE agreeing to produce, display or otherwise assist with the Video, the Author hereby grants to JoVE, subject to **Section 7** below, the exclusive, royalty-free, perpetual (for the full term of copyright in the Article, including any extensions thereto) license (a) to publish, reproduce, distribute, display and store the Video in all forms, formats and media whether now known or hereafter developed (including without limitation in print, digital and electronic form) throughout the world, (b) to translate the Video into other languages, create adaptations, summaries or extracts of the Video or other Derivative Works or Collective Works based on all or any portion of the Video and exercise all of the rights set forth in (a) above in such translations, adaptations, summaries, extracts, Derivative Works or Collective Works and (c) to license others to do any or all of the above. The foregoing rights may be exercised in all media and formats, whether now known or hereafter devised, and include the right to make such modifications as are technically necessary to exercise the rights in other media and formats. For any Video to which this Section 6 is applicable, JoVE and the Author hereby grant to the public all such rights in the Video as provided in, but subject to all limitations and requirements set forth in, the CRC License.

7. Government Employees. If the Author is a United States government employee and the Article was prepared in the course of his or her duties as a United States government employee, as indicated in **Item 2** above, and any of the licenses or grants granted by the Author hereunder exceed the scope of the 17 U.S.C. 403, then the rights granted hereunder shall be limited to the maximum rights permitted under such statute. In such case, all provisions contained herein that are not in conflict with such statute shall remain in full force and effect, and all provisions contained herein that do so conflict shall be deemed to be amended so as to provide to JoVE the maximum rights permissible within such statute.

8. Likeness, Privacy, Personality. The Author hereby grants JoVE the right to use the Author's name, voice, likeness, picture, photograph, image, biography and performance in any way, commercial or otherwise, in connection with the Materials and the sale, promotion and distribution thereof. The Author hereby waives any and all rights he or she may have, relating to his or her appearance in the Video or otherwise relating to the Materials, under all applicable privacy, likeness, personality or similar laws.

9. Author Warranties. The Author represents and warrants that the Article is original, that it has not been published, that the copyright interest is owned by the Author (or, if more than one author is listed at the beginning of this Agreement, by such authors collectively) and has not been assigned, licensed, or otherwise transferred to any other party. The Author represents and warrants that the author(s) listed at the top of this Agreement are the only authors of the Materials. If more than one author is listed at the top of this Agreement and if any such author has not entered into a separate Article and Video License Agreement with JoVE relating to the Materials, the Author represents and warrants that the Author has been authorized by each of the other such authors to execute this Agreement on his or her behalf and to bind him or her with respect to the terms of this Agreement as if each of them had been a party hereto as an Author. The Author warrants that the use, reproduction, distribution, public or private performance or display, and/or modification of all or any portion of the Materials does not and will not violate, infringe and/or misappropriate the patent, trademark, intellectual property or other rights of any third party. The Author represents and warrants that it has and will continue to comply with all government, institutional and other regulations, including, without limitation all institutional, laboratory, hospital, ethical, human and animal treatment, privacy, and all other rules, regulations, laws, procedures or guidelines, applicable to the Materials, and that all research involving human and animal subjects has been approved by the Author's relevant institutional review board.

10. JoVE Discretion. If the Author requests the assistance of JoVE in producing the Video in the Author's facility, the Author shall ensure that the presence of JoVE employees, agents or independent contractors is in accordance with the relevant regulations of the Author's institution. If more than one author is listed at the beginning of this Agreement, JoVE may, in its sole discretion, elect not take any action with respect to the Article until such time as it has received complete, executed Article and Video License Agreements from each such author. JoVE reserves the right, in its absolute and sole discretion and without giving any reason therefore, to accept or decline any work submitted to JoVE. JoVE and its employees, agents and independent contractors shall have

jove JOURNAL OF VISUALIZED EXPERIMENTS
1 Alewife Center #200
Cambridge, MA 02140
tel. 617.945.9051
www.jove.com

ARTICLE AND VIDEO LICENSE AGREEMENT

full, unfettered access to the facilities of the Author or of the Author's institution as necessary to make the Video, whether actually published or not. JoVE has sole discretion as to the method of making and publishing the Materials, including, without limitation, to all decisions regarding editing, lighting, filming, timing of publication, if any, length, quality, content and the like.

11. Indemnification. The Author agrees to indemnify JoVE and/or its successors and assigns from and against any and all claims, costs, and expenses, including attorney's fees, arising out of any breach of any warranty or other representations contained herein. The Author further agrees to indemnify and hold harmless JoVE from and against any and all claims, costs, and expenses, including attorney's fees, resulting from the breach by the Author of any representation or warranty contained herein or from allegations or instances of violation of intellectual property rights, damage to the Author's or the Author's institution's facilities, fraud, libel, defamation, research, equipment, experiments, property damage, personal injury, violations of institutional, laboratory, hospital, ethical, human and animal treatment, privacy or other rules, regulations, laws, procedures or guidelines, liabilities and other losses or damages related in any way to the submission of work to JoVE, making of videos by JoVE, or publication in *JoVE* or elsewhere by JoVE. The Author shall be responsible for, and shall hold JoVE harmless from, damages caused by lack of sterilization, lack of cleanliness or by contamination due to the making of a video by JoVE its employees, agents or independent contractors. All sterilization, cleanliness or decontamination procedures shall be solely the responsibility of the Author and shall be undertaken at the Author's expense. All indemnifications provided herein shall include JoVE's attorney's fees and costs related to said losses or damages. Such indemnification and holding harmless shall include such losses or damages incurred by, or in connection with, acts or omissions of JoVE, its employees, agents or independent contractors.

12. Fees. To cover the cost incurred for publication, JoVE must receive payment before production and publication the Materials. Payment is due in 21 days of invoice. Should the Materials not be published due to an editorial or production decision, these funds will be returned to the Author. Withdrawal by the Author of any submitted Materials after final peer review approval will result in a US$1,200 fee to cover pre-production expenses incurred by JoVE. If payment is not received by the completion of filming, production and publication of the Materials will be suspended until payment is received.

13. Transfer, Governing Law. This Agreement may be assigned by JoVE and shall inure to the benefits of any of JoVE's successors and assignees. This Agreement shall be governed and construed by the internal laws of the Commonwealth of Massachusetts without giving effect to any conflict of law provision thereunder. This Agreement may be executed in counterparts, each of which shall be deemed an original, but all of which together shall be deemed to me one and the same agreement. A signed copy of this Agreement delivered by facsimile, e-mail or other means of electronic transmission shall be deemed to have the same legal effect as delivery of an original signed copy of this Agreement.

A signed copy of this document must be sent with all new submissions. Only one Agreement required per submission.

CORRESPONDING AUTHOR:

Name: Arlette Kolta

Department: Département de Neurosciences

Institution: Université de Montréal

Article Title: Methods to analyze size, shape and directionality of networks of coupled astrocytes.

Signature: 

Date: 03/05/2018

Please submit a signed and dated copy of this license by one of the following three methods:

1) Upload a scanned copy of the document as a pfd on the JoVE submission site;
2) Fax the document to +1.866.381.2236;
3) Mail the document to JoVE / Attn: JoVE Editorial / 1 Alewife Center #200 / Cambridge, MA 02139

For questions, please email submissions@jove.com or call +1.617.945.9051

Click here to download Rebuttal Letter Rebutal letter JoVE Condamine et al.docx

We thank the editor and the reviewers for their detailed examination of the manuscript. We have considered every one of their comments and made corrections accordingly when possible. Please find below our reply (in red, and preceded by "Re:") to each of these comments. We hope that you will find this much improved manuscript suitable for publication.
Sincerely,
Arlette Kolta (Senior author)

Editorial comments:
Changes to be made by the Author(s):

1. Please take this opportunity to thoroughly proofread the manuscript to ensure that there are no spelling or grammar issues. The JoVE editor will not copy-edit your manuscript and any errors in the submitted revision may be present in the published version.
Re: Done

2. Please ensure that the references appear as the following: [Lastname, F.I., LastName, F.I., LastName, F.I. Article Title. Source. Volume (Issue), FirstPage – LastPage, doi: DOI (YEAR).] For more than 6 authors, list only the first author then et al.
Re: Done

3. Please define all abbreviations before use.
Re: All the abbreviations are defined at first use

4. Please use focused images of uniform size/resolution (at least 300 dpi).
Re: Ok

5. Please revise the table of the essential supplies, reagents, and equipment. The table should include the name, company, and catalog number of all relevant materials in separate columns in an xls/xlsx file.
Re: Done

6. Please provide an email address for each author.
Re: Done

7. Please rephrase the Summary to clearly describe the protocol and its applications in complete sentences between 10-50 words: "Here, we present a protocol to …"
Re: The summary has been rephrased accordingly

8. Please ensure that the Abstract is between 150-300-word limit.
Re: The abstract contains 300 words.

9. Please adjust the numbering of the Protocol to follow the JoVE Instructions for Authors. For

example, 1 should be followed by 1.1 and then 1.1.1 and 1.1.2 if necessary. Please refrain from using bullets or dashes.
Re: The numbering of the protocol has been modified

10. Please leave a single line space between each numbered step, sub-step and notes of the protocol.
Re: Done

11. Please revise the text to avoid the use of any personal pronouns (e.g., "we", "you", "our" etc.).
Re: Done. There are no personal pronouns in the Protocol section of the text

12. Please ensure that all text in the protocol section is written in the imperative tense as if telling someone how to do the technique (e.g., “Do this,” “Ensure that,” etc.). The actions should be described in the imperative tense in complete sentences wherever possible. Avoid usage of phrases such as “could be,” “should be,” and “would be” throughout the Protocol. Any text that cannot be written in the imperative tense may be added as a “Note.” However, notes should be concise and used sparingly. Please include all safety procedures and use of hoods, etc.
Re: The text has been modified accordingly

13. The Protocol should contain only action items that direct the reader to do something.
Re: The Protocol have been modified accordingly

14. Please add more details to your protocol steps. Please ensure you answer the “how” question, i.e., how is the step performed?/ Alternatively, add references to published material specifying how to perform the protocol action.
Re: More details have been added to the Protocol

15. 110: How do you anesthetize? What concentration? What animal is used? Age, sex strain specific bias? How do you perform the brain removal?
Re: These precisions are now given in the text

16. 112: Do you isolate whole brain? Do you remove extra tissues surrounding it?
Re: Details were added to the text.

17. 112: What is the area of interest that is being dissected and how? Please provide details.
Re: Here, the area of interest is the brainstem. Details were added to the text, but it should be kept in mind that the described method is valid for all other areas as well.

18. 162-172; 250-272: We cannot have paragraphs of text in the protocol section. Please consider moving to the discussion section or convert it to substeps in imperative tense.
Re: The text has been converted to substeps in imperative tense.

19. After all the formatting and changes, please ensure that the protocol is no more than 10-page.
Re: The protocol does not exceed 10 pages

20. Please ensure that the highlight 2.75 pages or less of the Protocol (including headings and spacing) that identifies the essential steps of the protocol for the video, i.e., the steps that should be visualized to tell the most cohesive story of the Protocol. The highlighted steps should form a cohesive narrative with a logical flow from one highlighted step to the next. Remember that non-highlighted Protocol steps will remain in the manuscript, and therefore will still be available to the reader.
Re: Done

21. Please obtain explicit copyright permission to reuse any figures from a previous publication. Explicit permission can be expressed in the form of a letter from the editor or a link to the editorial policy that allows re-prints. Please upload this information as a .doc or .docx file to your Editorial Manager account. The Figure must be cited appropriately in the Figure Legend, i.e. "This figure has been modified from [citation]."
Re: This information will be uploaded as a doc file as requested

22. As we are a methods journal, please revise the Discussion to explicitly cover the following in detail in 3-6 paragraphs with citations:
a) Critical steps within the protocol
b) Any modifications and troubleshooting of the technique
c) Any limitations of the technique
d) The significance with respect to existing methods
e) Any future applications of the technique
Re: Those points are now covered in the discussion.

Reviewers' comments:

Reviewer #1:
Manuscript Summary:
Condamine and colleagues describe a method to assess astrocytic connectivity through dye-coupling and Image-J. Indeed, a proper measurement of functional connectivity would be very beneficial to the scientific community.

Major Concerns:
No major concerns

Minor Concerns:
-Page 2, line 50 "astrocytes .....and are activated by K+ released during neuronal firing." –
Astrocytes are not "activated" by K+, rather clear it from the extracellular matrix once concentration exceeds a certain limit, see Bellot-Saez et al

https://doi.org/10.1016/j.neubiorev.2017.03.002
Re: This part of the sentence has been deleted

-page 3, line 106, "slice holder", should be "slice incubation chamber" or "slice recovery holding chamber".
Re: Text corrected in pages 2-3, lines 123 to 138

The authors should also relate to recent development in the field that allow prolonged incubation.
Re: A note was added at 1.12 regarding this

-The authors apply the biocytin for 30 min, which probably diffuse into astrocytes that are not directly connected to the recorded astrocytes. This should be discussed.
Re: The 30 min application starts after the cell is patched. It is unclear why biocytin should diffuse into unconnected cells. In Condamine et al., Glia (2018), we compared labelings obtained with biocytin applications for 30min and 1 hour and found no difference arguing against the point raised by the reviewer. Nevertheless, text was added to the discussion with regard to this comment (page 15, lines 642-645).

The "subtract background" tool is fundamental to this process, and must be constant, otherwise it may lead to bias of the results... please discuss
Re: the "subtract background" tool is constant; it is only adjusted in cases of very strong deposits of biocytin in the area of the patched cell.

Reviewer #2:
Manuscript Summary:
Condamine et colleagues detail a method to describe spatial organization of astroglial network within a specific brain structure using brain slices and image processing with ImageJ, Excel and Adobe Illustrator. They use their own ex vivo data to illustrate the procedure : experiments were performed in slices from the dorsal part of the trigeminal main sensory nucleus (NVsnpr), an area involved in masticatory movements, which is a well studied by A. Kolta's laboratory (Morquette et al. 2015, Condamine et al. 2018, etc).
While part of the procedures is relatively classic (detection of astroglial network using dye coupling in slices, count of loaded cells, detection of 2D size of the astroglial networks), Condamine et colleagues also developed a quantification allowing comparisons of putative preferential orientation of astroglial networks, which is a new and a very interesting tool allowing the study of astroglial coupling dynamics. This approach could be useful in various conditions, ranging from physio- to physiopathological states.
The paper is well written and the procedure is clear. Step-by-step instructions can be followed with no major difficulties. Of note, experimental data used to illustrate the procedure have been already published in Glia (2018).

Major Concerns (relative to the yellow section):

*A summary is needed for the "image analysis" section.
Authors should summarize briefly image processing at the beginning of the "image analysis" section (l. 173) to favor understanding of the global procedure.
Re: It is against JoVE's instructions to have paragraphs of text in the protocol section. The protocol has to be described step by step in bullet form.

* Condamine et al. Glia (2018).
It should be clearly mentioned, in the main text, that data and image processings are already published in Glia in 2018. Authors only mention it in figure legends.
Re: Condamine et al. Glia (2018) is now mentioned at the beginning of the representative results section.

* Free software.
It would be great to avoid the use of commercial software (illustrator or excel) and promote the use of free softwares (such as inskape, Calc, …). First of all, formulations such as "vector image editor" and "spreadsheet application" should be preferred to commercial software names, and commercial names should be only cited as examples. Secondly, might authors translate adobe illustrator commands in inscape commands?
Re: We corrected and used the formulations proposed and cited the commercial software names in example. As for the command regarding Adobe Illustrator, we are not aware of how to proceed with the reviewer's suggestion.

*Simplified processes.
Authors should improve some procedures.
First, image processing in section 6.5 can be performed on image J. (Thus, the use of Adobe Illustrator seems not required).
-4x image can be resized in Image J (process=> Adjust => size), and save in .TIFF in image J.
-the coordinate called "20x referential point" can then be determined in image J: when you deplace the cursor mouse in the resized 4x, the coordinates of the cursor mouse position (x =, y =, and also the intensity value of the pixel = …) are written on the left-bottom corner in the main Image J toolbar.
Re: The procedure suggested by the reviewer does not allow us to determine the left top corner of the 20X image named "20X referential point" in the 4X image. The main interest to use a vector image editor was to superpose the 20X image on the 4X image and align them by using an opacity tool like the one in Adobe Illustrator CS4 to adjust the transparency of the 20X image and align it on the 4X image.

Secondly, could authors explain the relevance of determining both the coordinates of the 20x image in the "4x resized image" and the coordinates of the 20x image in the brain structure image (after the use of rectangle bounding option) for the positioning of the loaded network in the brain structure. Is the step "positioning in the "4x resized image" really needed (section 6.5)? If so, authors should explain why it is not a redundant procedure.
Re: Yes the step "positioning in the "4X resized image" is really needed because this image is used to determine the position and the coordinates of the bounding rectangle surrounding the

NVsnpr. The coordinates of each cell of a network was first determined in the 20X image, but we needed to translate them into the 4X image referential in order to report them in the bounding rectangle referential (used for population data).

Finally, it might be interesting for readers to know that Image J can process calculations (using macros), and that the used of Excel is likely not required to translate cells coordinates.
Re: This is an interesting suggestion, but a spreadsheet application is more user friendly.

*Alternatives
Authors should give alternatives to their procedures, when appropriate.
For example,
- The "cell counter" pluggin allow manual detection on raw z-stack image. I agree that it is not an automatic detection, but sometimes "analyze particule" is difficult to perform or prone to errors. Authors might mention cell counter pluggin as a good alternative (or to double check).
Re: We tried using the "cell counter" pluggin for the work published in Condamine et al. (Glia 2018) and found that, since this is a manual method, it is really prone to experimenter bias. However, we added a sentence mentioning that a cell counter pluggin can be used when labeling is unequivocal.

- Watersheld is not always appropriate (as mentioned by authors in discussion), and can easily lead to overestimation. Drawing a white line between fused cells is some time more efficient to dissociate cells.
Re: Watershed draws a white line of 1 pixel thickness between two close objects on a binary file. We wrote to use the watershed option only when necessary: page 7 lines 292-294 “If a group of 2 or more labeled cells in the network are detected as a single cell with the Analyse Particles tool, because they are too close to each other use the Watershed tool”. Moreover, we had already added a “warning” in the discussion regarding use of this tool “Another limitation of the method described is the “watershed” tool used to discriminate cells that are too close to each other. Visual inspection of detected cells should be done when using this tool.”

- It might be mentioned that SR101 loading is not required to p identify astrocyte in slices for patch-clamp recordings.
Re: A ramp and a step IV protocol were used to identify astrocytes on the basis of their electrophysiological properties, but SR-101 loading (Kafitz et al., 2008) is really useful to target astrocytes for patch-clamp recording. A sentence was added at the beginning of step 3 to mention that.

* Pixels or µm?
Is the use of images scaled "in pixel" required or could the global process being fully achieved with images already scaled in "µm"? If "pixel scaling" is required, then authors might indicate how to switch between pixel and µm in the section "preparation of data" section (l. 174). (image => properties: choose then "pixel" with "1" for pixel dimension).
Re: We use pixel unit in all the process and convert the measure in µm at the end. We choose this method to avoid conversion problems if the data set is not imaged with the same

microscope for example. We added a sentence about pixel scaling into the section "preparation of data".

*Relevance of vector size: Is a small vector really indicate a preferential orientation? The size of the vector (for each network) indirectly informs on the strength of the preferential orientation of the astroglial network, independently of the cells number within the network. Thus, the size of the vector matter, and can give substantial informations. However, this is not mentioned by authors. To my opinion, this is a major limit of the detailled method in the manuscript.
Which factors influence vector size (density of cells, spatial orientation...) ? What type of informations are provided by vector size ? How such information can be used for comparison of astroglial networks? What is the limit (Is a small vector really indicate a preferential orientation?)? Authors should clarify this in the main text and/or ideally discuss its importance in the discussion section and/or add a complement of procedure for a comparison between astroglial networks.
Re: The reviewer is correct by assuming that a small vector indicates that there is no clear "dominant" or preferential orientation (independently of the cells number within the network). It will be mostly influenced by the spatial location of each cell in the network in relation to the patched astrocyte. We agree that smaller vectors do not reflect a strong preferential orientation, but still they reflect one direction. When is it too small to count? We prefer to not set limits and instead use the mean values. This information is still useful when comparing 2 conditions (like sensory stimulation vs Ca^{2+}-free medium, for example). A sentence was added to the discussion to stress the importance of vector size.

Minor Concerns:
- L.31 Authors referred to "density of the network" in the introduction, but never quantify it further. this should be clarified.
Re: Due to this misunderstanding, we removed this expression.

- For figures: Scale bars are in µm on figures. This is confusing, because all the procedure is performed in pixel. Authors should remove the "100 µm" in scale bars from figures, calibration of scale bars could however be indicated in the figure legend (pixels or equivalent in µm).
Re: All the analysis was performed in pixel and all the numeric data was converted in µm at the end. To us, it makes much more sense to provide the reader with a measure in µm, which is more meaningful. However, the figure has been corrected as requested.

- L.32: "4/ repositioning of the network within the area of interest" is not clear.
Re: Area of interest means a nucleus or a studied area of the brain. We use a general term to illustrate the use of this protocol.

- L. 53: Authors should to choose between « etc » or « … ».
Re: Corrected

- L.105: The "perfusing buffer" is also used for slice storage (not only for patch-clamp and dye coupling).
Re: Corrected

- L.109: the tubing in the storage chamber is required for carbogen (95 % O2 -5% CO2), not only for oxygen delivery.
Re: Text corrected (page 3 lines 113, 120 and 126)

- L.116: Authors should indicate how long slices have to stay in storage condition (aCSF, RT) before 34°C bath (for SR101 Loading). ~ at least 1 hour ? less ?
Re: Text corrected

- L.134: It should be also mentioned that astrocytes display, in general, a Vm around -80mV.
Re: In some brain structures like in NVsnpr astrocytes are more depolarized and showed a Vm around -70mV. It's the reason why we don't mention a general Vm.

L.141: Is the IV protocol (every 5 min) required to follow variation of Resistance input or is it performed to facilitate dye diffusion? This question should be addressed, considering the very low (leaky) membrane resistance of astrocytes.
Re: The IV protocol every 5 minutes is only required to facilitate biocytin diffusion.

- L.147: add "then" before "discard the case", to facilitate the reading.
Re: Corrected

- L.154: in the "4.biocytin relevation" section. One should always pay attention to the side of the slice, when mounting slices on coverslips. Indeed, the use of astrocyte patch-clamp for dye coupling experiments are usually performed in "surface" of the 350 µm-slice. The "loaded side" of the slide should be accessible for scanning confocal acquisition. If true for authors, this should be mentioned in the "4. biocytin revelation" section.
Re: Corrected. We added sentences to the text (in the "Astrocytes patching and filling with biocytin" section and the Biocytin revelation section) with regard to that comment.

- L.156: streptavidin without "-e"
Re: Corrected

- L.195: it's "make binary", not "make a binary".
Re: Corrected

- L.202: "In the setting "show"" is not clear (and not reported adequately in fig 3C). "Display results" will be probably more appropriate.
Re: Corrected.

- L.212: for a real unbiaised analysis, the "Watersheld" tool should be systematically used before the "analysis particule".
Re: ''Watershed'' process is only used when some cells are too close to be considered by the counting process. We didn't use this process systematically because it can increase the number of cell detected by dividing some cell in two different parts. We recommend visual inspection every time it is used.

- L.245: "draw a ROI at the patched cell location and add it to the ROI manager." might be clearer.
Re: Corrected

- L.268: it should be mentioned that the coordinate of the "reference cell" is not included. The length of the main vector is then divided by : the number of cells in the network - 1.
Re: Corrected

- L.286: "Select and hold the "pipette tool" to see "the measure tool" in the tools panel" might be clearer.
Re: Corrected

- L.385: Calcium free condition also increases neuronal activities (Morquette et al. 2015) and increase of neuronal activities might increase astroglial coupling. Thus, can the calcium free condition only be used to increase connexin permeability? Reformulation of this part could be required.
Re: We don't see how a stimulus can increase astroglial coupling without having an effect on connexins. The sentence states that we have used the Ca^{2+} free condition as a massive stimulus to open up the syncytium and maximize tracer diffusion through gap junctions (whether it's indirect through an effect on neurons or not is irrelevant).

- L432-438: there are not enough data (7C and 7D) to clearly access to sample distributions without over-interpretation. A "peak" can not be determined with n=2 networks. Student test cannot be used here (inequal variance, low sample size, Gaussian distribution not so clear…). Is there really a preferential orientation in 7B3 if you take into account the size of vectors? Is there a preferential orientation when data are distributed from 0 to 180°? Authors should reformulate with caution this part.
Re: These data have been published as they are and have already been reviewed for publication in Glia. We do not think there is over-interpretation. The data is not distributed equally from 0 to 180° as stated by the reviewer. In fact 6 of the 8 networks (with sensory stimulation) have a preferential orientation above 80°. The important point here is that an orientation towards the center would have been closer to zero as with the networks obtained under Ca^{2+}-free conditions. Obviously, all the networks obtained with sensory stimulation will not have a single dominant preferential orientation since the position of their starting point (the patched astrocyte) varies. We removed the reference to "peaks". As for the statistics, we systematically verify when a test can be used according to data distribution and sample size. In this case the normality test and the equal variance test were passed (with $p = 0.273$ and $p = 0.478$

respectively) and allowing for use of the student test. Both groups passed the Kolmogorov-Smirnov test assess normality (Sensory Stim: K-S Dist. = 0,174, P > 0,200; and Ca^{2+}-free: K-S Dist. = 0,272, P = 0,053).

- L.532: Why do authors believe that "the number of cells detected with this method is largely underestimated"? references with patch-clamp of neurons can be misunderstood. Thus, this first paragraph is confusing and should be clarified.
Re: The reasons why we believe that the number of cells are underestimated is clearly stated in the text. In many types of coupled cells (not just neurons) there are evidence on the basis of electrophysiological recordings that dye coupling does not always occur between coupled cells. Many examples are from studies on neurons, but it is also the case of other types of cells and there is no reason to believe why it would be different for astrocytes.

- L.532: To my opinion, It should be clearly stated that the number of loaded cells depend, at first, of the time used during experiment to load the patched cell.
Re: To avoid variability, 30 minutes was the time systematically used for loading, and as stated above, in Condamine et al, Glia (2018) we compared loadings of 1 hour and 30 min and found no differences.

- Authors should precise what is the Iman-Conover methods (2 way ANOVA on ranks) and which software has been used for statistics.
Re: There is no section for statistics in JoVE. We do not know where to add that.

- material : change "VT100S" with "VT1000S".
Re: Corrected

Reviewer #3:
Manuscript Summary:
In the study entitled "Methods to analyze, shape and directionality of networks of coupled astrocytes" a ImageJ/FIJI-based analysis of gap junctional coupling of astrocytes in the trigeminal nucleus is described. Sulforhodamine 101-labeled astrocytes in acute tissue slices were patch-clamped and dialyzed with biocytin to mark coupled cells. After labeling of coupled cells the cell number, the network area and the preferential orientation of dye spreading was determined using ImageJ/FIJI. The semi-automated analysis provides more objective results compared to earlier studies that rely on manually evaluated networks. However, this study suffers from a couple of weaknesses (see comments below) and needs to be thoroughly revised. In particular, the post hoc identification of the patched cell and the lack of a critical discussion of advantages/disadvantages of this method compared to other methods is a matter of concern.

Major Concerns:
1. In chapter 3 (Astrocyte patching) fundamental information is missing:

A paragraph has been added to describe the patch procedure in details. This was first omitted because the paper's focus is on methods to assess astrocytic networks, rather than electrophysiological recordings.

a. What is the sampling rate of the whole-cell recordings?
Re: The sampling rate was 10kHz. This has been added to the text.

b. Was the liquid junction potential corrected?
Re: We added a sentence with a reference for a method to correct for LJPs when needed. Liquid junction potentials will vary greatly with internal and external solutions used for recordings which are likely to differ with the type of experiment being conducted. They are important to determine for experiments involving ion channel selectivity or when precise voltage commands are administered, and importantly, they are likely to change in the course of a recording session if the bath solution changes or during a prolonged recording from a cell. Therefore, we did not put emphasis on correcting LJP here since voltage measurement and commands were not strictly important. In the experiments described here we corrected the offset before seal formation and subtracted any value that appeared at the end of the recording after retracting from the cell.

c. Were traces online or offline filtered?
Re: Traces were filtered online at 1KHz.

d. Were patches compensated for fast and slow capacitance and series resistance?
Re: Yes

2. Yes, "in most cases, the patched astrocyte shows the stronger labelling than the adjacent the adjacent cells stained through tracer coupling" (L235-236). This is a rather shaky way of determining the origin of the network. It is better to use a predominantly gap-junction impermeable and fixable fluorescent dye that does not interfere with the biocytin labeling fluorophore. In this case, Alexa Fluor 488 would be suitable. Then you can be sure that you can unerringly identify the patched cell. The corresponding discussion section (L564-569) suggests that this improvement is somehow difficult, which is not the case (cf. Augustin et al., 2016, Glia).
Re: The reviewer is correct about the fact that adding a dye to the recorded cell. Alexa 488 crosses gap junctions in our hands and is not fixable. However, we changed the text and now propose to add Dextran, which resist fixation and do not cross GJ when large enough.

3. As there are patched cells lost eventually upon withdrawal the pipette, the capability to determine reliably the origin of the reconstructed network is lost as well. In order to save the maximum of results/data the authors calculate the putative position of the patched cell (section 6.4.1). However, you cannot be absolutely confident about the position of the lost cell thereby challenging all analyses that depend on that information. It is better to omit such experiments from e.g. the vector analysis. However, it is still possible to use respective experiments for the analysis of network area and cell number (if you add +1 in the latter case to account for the lost cell).

Re: The location of the initial biocytin deposit is very clear most of the time and is usually quite limited so that it will not affect the vector analysis dramatically. Since, loss of the patched cell is common, removal of all cases where it happens would reduce the sample size significantly. However, the reviewer's suggestion is a possibility that can be considered and is now added as an alternative option in the text.

4. Astrocytes and oligodendrocytes form panglial networks in many brain regions (Maglione et al., 2010, Glia; Griemsmann et al., 2015, Cereb Cortex; Augustin et al., 2016, Glia; Moshrefi-Ravasdjani et al., 2017, Neurochem Res; Claus et al., 2018, Cereb Cortex). Are all coupled cells really "labelled astrocytes" (L387)? If it cannot be proven somehow, it must they must be called "labelled cells" (L378). See also L509.
Re: The reviewer is absolutely correct about this. Corrections have been made accordingly.

5. In section 4 "Biocytin revelation", fluorescent labeling of biocytin via streptavidin is described (L154-161). However, Figure 6C middle (0 Ca2+ experiment) shows DAB labeling. The latter method is not mentioned in section 4. Regarding the shown quantification and comparison of coupled cells and covered area (Figure 6D-E) it is fundamental to use only one method. It is likely, that DAB reaction stronger labels cells that would have been below detection threshold using streptavidin conjugated with a fluorophore. Comparison with other experimental configurations (Ctrl, fiber tract stimulation and CBX in 0 Ca2+) is not valid.
Re: We disagree that the DAB reaction gives stronger labeling. In fact, we used DAB in the beginning for that reason specifically, but on comparisons with labelings obtained with Streptavidine, we found no differences. Details about the DAB revelation are now added to the methods and an advice against using different methods is also given. However, we think it remains an interesting option that experimenter should be aware about if they cannot use fluorescence.

6. It is stated that preferential direction of dye spread is only addressed in one other study (Houades et al., 2008; J Neurosci). However, that is not the current knowledge. Preferential dye spreading has been investigated in the hippocampus (Houades et al., 2006, Neuron Glia Biol; Rouach et al., 2008, Science; Anders et al., 2014, Philos Trans R Soc Lond B Biol Sci), the cortex (Houades et al., 2006, Neuron Glia Biol), the glomerulus (Roux et al., 2011, Proc Natl Acad Sci U S A), the thalamus (Claus et al., 2018, Cereb Cortex), and the lateral superior olive (Augustin et al., 2016, Glia).
Re: Again, the reviewer is absolutely right about these previous findings. These are now mentioned in the introduction and the discussion.

7. It should be discussed what the advantage/disadvantage of the present method is compared to the methods used in the literature listed above (#6).
Re: The main advantage of our method is that it provides for a mean to describe the organization and orientation of astrocytic networks in structures like the dorsal trigeminal main sensory nucleus that are not known to have a precise organization. In all of the above studies, the networks orientation is described in relationship to the shape of the structure itself which is already documented (e.g. the barreloid in the thalamus, the barrels in the cortex, the layers in

the hippocampus and cortex, the glomeruli in the olfactory bulb...etc). In addition, our vectorial analysis enabled us to detect that coupling orientation may vary with conditions (e.g. when comparing orientation preference observed with zero Ca^{2+} vs with sensory fiber stimulation). This advantage is now added to the discussion.

Minor Concerns:

1. Stick to one name of the software: ImageJ vs. ImageJFIJI (e.g. L29+240 vs. L175).
Re: Corrected with ImageJFIJI

2. In L37-38, why not define the (trigeminal) nucleus instead of staying unspecific?
Re: Corrected

3. The list of putatively benefitting nuclei (L42-43) should be extended by the auditory brainstem, which is spatially rather close to the trigeminus. In the lateral superior olive glial networks exhibit a specialized topography (Augustin et al., 2016, Glia).
Re: Corrected

4. Consider adding the review by Verkhratsky and Steinhäuser, 2000, Brain Research Reviews (L50).
Re: Added

5. Unconventional list. Please modify and add a suitable citation preferentially another review (L53).
Re: References added

6. Specialized gap junctional coupling is named for barrel cortex and olfactory bulb (L60-68). In addition, a link to another sensory system, i.e. the lateral superior olive within the auditory brainstem (Augustin et al., 2016, Glia), which is spatially close to the trigeminal nucleus, should be given.
Re: Corrected

7. Consider citing Ref. #6 at the end of sentence (L71).
Re: Corrected

8. The x/y ratio as a mean to describe network topography was not exclusively used in the barrel cortex (L82-85), but as well in the hippocampus and the lateral superior olive (Houades et al., 2006, Neuron Glia Biology; Augustin et al., 2016, Glia). Consider addition of this information for a more comprehensive view.
Re: Corrected

9. Typo: "SR-101" (L121).
Re: Corrected

10. Room temperature was defined as "RT" (L115). Use it accordingly (L122).

Re: Corrected

11. Typo: "SR101 labelled" vs. "SR101-labeled" (L130). See also L448.
Re: Corrected

12. Check correct usage of hyphens: e.g. "voltage-clamp" (L134), "whole-cell current-voltage protocoll" (L135), "current-clamp" (L137). See also L446 ("patch-clamp").
Re: Corrected

13. Define step size for current-clamp protocol (l138).
Re: We performed steps of 100pA. This was added to the text

14. L206: add "(3C, left part)" at the end of the sentence.
Re: Corrected

15. L226: add "Figure 4B"
Re: Corrected

16. L227: Wrong figure reference: It must read "Figure 4B".
Re: Corrected

17. Depending on the confocal system, the Meta data already contain the conversion factor for the microscope. Thus, FIJI already uses µm scaling, e.g. when processing pictures taken at a Leica LSM SP5. This possibility has to be mentioned in order to avoid confusion.
Re: we mention that we only work in pixels with imageJFIJI and check the setting for this (line 259)

18. In section 6.4.2 the new referential coordinates are given as " x', y' " (L255-258). In section 6.4.3 the coordinates of the cells are given as " x1, x2 " etc. (L265-267). Here, one should better write " x'1, x'2 " etc. (accordingly for y coordinates) to be not confused with the coordinates " x, y " from the initial FIJI analysis.
Re: Corrected

19. In Figure 5 the labeling of axes is heterogeneous (regarding spaces). At the arrows indicating orientation it must read "Medial". In L344 it must read "lateromedial" and "dorsoventral". See also Figure 7.
Re: Corrected

20. L275: Specify Adobe Illustrator version. There arrangement of controls might be heterogeneous across different Adobe Illustrator versions.
Re: We used CS4 version. Added to the text.

21. To account for left-right orientation it is suggested to recalculate x coordinates (L327-331).

Why not just mirroring the picture in FIJI before starting the analysis? Then one has not to perform another calculation.
Re: Interesting suggestion. We added it to the text.

22. L353: To avoid confusion specify which part of the formula is covered by the square root, e.g. by adding another pair of brackets.
Re: Corrected

23. Consider indicating that CBX was used in an independent set of experiments (L374-378).
Re: Specified as requested

24. Figure7: Bars in panels C and D are not aligned and do not optically fit to the binning mentioned in the text (L434+436). I suspect that the bars were misaligned during the design process in the graphic software. This should be corrected.
Re: Figure has been corrected and the text was modified du to another comment.

Reviewer #4:
Manuscript Summary:
Methods are given for measuring the extent of tracer coupling of astrocytes and applied to the MesV sensory nucleus. The coupling is blocked by carbonoxylone, a well know blocker of gap junctions. Extent of coupling is altered by sensory stimulation and by placing in low Ca solution. That's good, but haven't they already published that?
Re: The reviewer is clearly aware of our very recent publication (in Glia) regarding astrocytic networks in the Main (and not MesV) sensory nucleus. The present article was written following an invitation from JoVE to describe in greater detail the methods used in this recent publication.

Major Concerns:
A) The depth dimension of the coupled domains is not analyzed. B) If the labeled cells constituted a compartment, the vector of the coupling would depend on which cell was injected. C) There is no convincing evidence that the limit of tracer spread is not simply a matter of drop off with distance of concentration to the threshold of their method.
Re: A) The depth dimension beyond the limit of the Z stack is not analyzed because of the limits imposed by the fact of working in slices. We assume that cells at the surface of the slice (on each side) and their processes are damaged, leaving only the middle part of the slice intact. Cells in that region are presumably encompassed in networks revealed with Z-stacks, but given the narrowness of this region and the slight variability in cutting angles from one animal to the other, we collapsed the Z stack in 2D.

B) Indeed, the vector of coupling is expected to depend on the position of the injected cell within the network. This is exactly why we developed these elaborate calculations.

C) If this were the case, tracer spread would be similar under all conditions and we would not have more labeling under one condition (low calcium) vs the other (sensory stimulation). In

addition, in experiments using the exact same methodology, but in the visual cortex for a different project, we reveal much larger networks with much more extensive tracer spread (unpublished results), suggesting that it is not a limit of the method but rather a limit of the networks being investigated.

We have no idea whether coupling domains overlap or whether the whole nucleus could be one domain. You could develop and use a technique for multiple injections (at least 2) and tracers of different colors. Are the domains volume filling of the space between neurons? There is reason the think that single astrocytes interdigitate to only a small degree.
Re: The reviewer's comment is relevant for interpretation of the data rather than the methods. Whether astrocytic coupling domains overlap or not is important to understand the function of the circuitry. Here we only report about the methods used to describe a domain. The question raised by the reviewer is beyond the scope of this methodology paper. Secondly, according to some, introduction of a tracer in a cell often interferes with labelling by another tracer; although this is something that we have not validated ourselves.

One would have liked some consideration of the dye coupling as a function of GJ permeability.
Re: A sentence regarding tracers permeating GJ have been added to the discussion

Admittedly not easy to measure in networks, but fundamental to the observations. If the tracer, e.g., biocytin is not destroyed in the cells and does not leak out, the coupling coefficient is unity given enough time. The vector of tracer coupling always points away from the injected cell. That makes it a not very important parameter functionally. Indeed coupling might drop off towards the edge of the nucleus (and it would have been interesting to make some measurements just outside of the border of the nucleus.
Re: We do not understand the point that the reviewer is trying to make with this comment and do not know how to address it clearly. Of course the vector of tracer coupling will always point away from the injected cell, but if the network is not confined within a structure, it will point in any direction and there would be no clear preferential orientation, even when the injected cell is near the border of the nucleus. This is not the case here, when cells near the border are injected, the preferential orientation of the network points towards the center of the nucleus and very rarely do we get tracer spread outside of the nucleus. In addition, we did carry out injections of cells in the ventral part of the nucleus (which correspond to a different area functionally) and obtained large networks that spread outside of the nucleus. These results are not presented here because again this is a method paper and not a paper to discuss the concept of astrocytic network domains.

The literature contains lots of pictures of dye filled cells with labeled processes. Why not here?
Re: The labelling reported here is comparable with that reported in most other articles using the same techniques. Moreover, visualization is done at low magnification to capture the entire network and this does not allow visualization of fine processes.

The techniques are of some interest and the change in tracer coupling with CBX and low Ca also. But we are left with many questions about the extent of coupling, questions that could be resolved with not much refinement of the methods.
Re: The reviewer did not spell out the questions to be addressed exactly. These questions are maybe addressed in our previous publication in Glia which reports about the findings and their functional significance. Here we limited the content to the methods used.

Minor points:
31. Define density? What about the z axis dimension?
Re: Density is the number of cells per μm^2. See reply above regarding the Z axis dimension

32. Explain somewhere how GJs can have a preferred orientation. "repositioning" means what?
Re: We never said that GJs have a preferred orientation. What we say is that there is a preferential orientation to tracer spread. This can happen because either: 1) only cells connected in a particular configuration are coupled through GJs, or 2) GJs are dynamically regulated. If the input regulating coupling is itself oriented (like is the case with the sensory fiber terminals for instance), then tracer spread across the regulated junctions will appear to have a preferential orientation.

Repositioning means to place back the reconstructed network within the nucleus or area of interest.

41. Are there functional domains? Hard to tell from single injections. Multiple injections might or might not show an edge of a domain.
Re: See reply above

50. activated ???
Re: This sentence was changed with regard to a comment raised by Reviewer 1 as well.

56. Are there restricted networks?
Re: Yes, according to our findings in Condamine et al, Glia, 2018, and to those of many others in the barrel cortex, the olfactory glomeruli, the barreloids in the thalamus, the lateral superior olive and the hippocampus (see reply to the comment below).

63. I don't think you mean "overlap neural compartments". They fill in lots of the space between neurons. The neurons may or may not be coupled by gap junctions to form compartments. In the barrel cortex, there is more astrocytic coupling within a barrel and less between barrels. Generally, astrocytes interdigitate very little with each other. How are the astrocytic networks oriented towards the center of the glomerula or of the barrel?
Re: We mean that in areas where neurons have a topographical organization, like in the Barrel cortex, astrocytic networks also display a structural segmentation that corresponds perfectly to the neural segmentation. The point that the reviewer is trying to make with the 2^{nd}, 3^{rd} and 4^{th} sentences of this paragraph is unclear. As for the last sentence, we only report about what has been previously published by others.

79. synchronized not very precise?
Re: We say synchronized and coordinated. What else could be more precise?

84. parallel to the surface is two axes.
Re: We changed the sentence.

87. preferred ???
Re: Preferred as in the dominant orientation reflected by the sum of vectors

90. a method to replace each network in reference to the boundaries of the nucleus ???
Re: See reply regarding “repositioning” the network above.

98. pretty low rate of cooling
Re: It may depend on the volume put to freeze. In any case it’s an approximate

113. plane of cutting? It's a long time before we find out.
Re: We do not understand what the reviewer wishes to address with this comment

123. How long can you keep the slices at room temperature?
Re: We keep brainstem slices easily for at least 8 hours. Others working on cortical or hippocampal slices can keep them for longer.

140. not positive to -60 mV
Re: Corrected

144. 15 min in addition to the 30 min for injection
Re: Yes. This is now specified

157. Alexa
Re: Corrected

167. "resolution of 800 by 800 pixels" What is the pixel size; what is the z dimension?
Re: The pixels size was 0.749µm.The z dimension was adjusted for all networks to allow getting the entire signal properly.

173 - 360. Who highlighted all this and why?
Re: This is requested by the journal for the video

185. Selection of the white outliers may be rather arbitrary.
Re: We are not sure to fully understand the question here. We remove « bright » outliers because we’re working against a black background.

195. The binary image obviously throws away a lot of data. Then there is the discard of small

spots. What is the criterion for a cell? What has happened to the cell processes that connect the cell somata?
Re: The binary image may throw away some data, but we think it is safer to underestimate the number of cells rather than counting artifacts and deposits as cells. The criterion for a cell are given in the section 6.2 just below this one. As for the processes, we do not consider that they should be counted as cells to avoid counting the same cell twice.

223. The surface area of the network as calculated excludes the cell processes on the edge of the network. What about the z axis extent of the network? Does this depend on the plane of section of the brain? Network area x/y extent can be close to section thickness.
Re: The surface area may be slightly larger if considering the processes, but the difference should not be significant and in any case, it can only be based on what is visible in the images. See the comment above regarding the Z axis. Depending on the area and the organization of astrocytic networks, their surface may vary with the plane of cutting and will obviously be limited by section thickness.

242. I see no strongly stained processes. Looks more like leakage. This measurement is before making the binary image.
Re: The sentence has been removed.

380. How do you get an area for a line connecting two cells?
Re: The area value given is an average value for all networks and not only those having 2 cells; and in the latter case, we draw an ellipse around the 2 cells and not a straight line.

390. In Fig. 6C 0 Ca image, why not biocytin fluorescence? Lots of leak?
Re: Just because, these were the first experiments conducted and we used DAB then. Later, we confirmed that equivalent results could be obtained in fluorescence, so we switched to fluorescence. There is not more leak on that image than on other images.

408. Fig. 6 D. Electrical stimulation still has an effect in the presence of CBX. Less marked for 0 Ca.
Re : It is probable that some labelling result from cells pumping biocytin that has leaked in the extracellular space. It is known that more active cells will pump more of the biocytin. An explanation for the data could be that electrical stimulation is more effective to activate the cells, whereas 0 Ca^{2+} only favors GJ opening.

Rebuttal Letter to editor

Click here to download Rebuttal Letter rebuttal letter to editor.docx

A1: The title matches the highlighted text.

A2: The citation has been added.

A3: Corrected.

A4: OK

A5: Yes. The information has been added in the text

A6: The information has been added in the text

A7: We converted part of the text into a note. We need to address the electrophysiological properties of the astrocytes in this part of the protocol. Theses characteristic are crucial to positively identify astrocytes.

A8: We corrected the text and removed the commercial name

A9: Corrected. We used 2 different mounting mediums depending on fluorescent revelation or DAB revelation. Specifications are provided in the Material table.

A10: We corrected the text and removed the commercial name

A11: This is already in the table of Material. We removed the commercial name from the text.

A12: We removed the commercial name from the text and added it in the table of Material.

A13: We removed the commercial name from the text and added it in the table of Material.

A14: OK

A15: A note has been added in the text

A16: This section has been rephrased

A18: We removed the commercial name from the text and added it in the table of Material.

A19: Corrected

A20: We meant the binary file or the detection file mentioned above in the protocol (step 6.1.8 or step 6.2.4, respectively). We corrected the text.

A21: The normalization of the nucleus as a rectangle is carried out by using the “Bounding Rectangle” measurement in ImageJFIJI. All the process is described in the following steps (6.5.2.2 to 6.5.2.4)

A22: OK

A23: OK

A24: The personal pronoun has been removed

A25: Steps 6.5.3.1 to 6.5.3.4. Added to the text.

A26: We converted this part to a note. The compilation of the data is realized by plotting the entire coordinates in percentage in a graph.

A27: We shortened the note and added a Supplementary Methods section to the manuscript.

A28: We compile all the angular differences by plotting them in vertical bar charts. We modified the text to clarify.

A29: Corrected with generic terms.

A30: We corrected the reference section. The option of “use full journal name” in the JoVE endnote style you provided was not quoted and don’t correct the problem. We had the journal title manually.

Supplemental File (Figures, Permissions, etc.)

Click here to download Supplemental File (Figures, Permissions, etc.) Copyright permission from Condamine et al. Glia 2017.docx

JOHN WILEY AND SONS LICENSE TERMS AND CONDITIONS

Jun 04, 2018

This Agreement between Mr. Steven Condamine ("You") and John Wiley and Sons ("John Wiley and Sons") consists of your license details and the terms and conditions provided by John Wiley and Sons and Copyright Clearance Center.

License Number	4296620242918
License date	Feb 26, 2018
Licensed Content Publisher	John Wiley and Sons
Licensed Content Publication	GLIA
Licensed Content Title	Functional rhythmogenic domains defined by astrocytic networks in the trigeminal main sensory nucleus
Licensed Content Author	Steven Condamine,Raphaël Lavoie,Dorly Verdier,Arlette Kolta
Licensed Content Date	Oct 23, 2017
Licensed Content Pages	16
Type of use	Journal/Magazine
Requestor type	Author of this Wiley article
Is the reuse sponsored by or associated with a pharmaceutical or medical products company?	no
Format	Electronic
Portion	Figure/table
Number of figures/tables	3
Original Wiley figure/table number(s)	Figure 1 , Figure 2, Figure 5
Will you be translating?	No
Title of new article	A method for astrocytic network analysis
Publication the new article is in	Jove
Publisher of new article	...
Author of new article	Condamine S, Verdier D, Kolta A
Expected publication date of new article	Apr 2018
Estimated size of new article (pages)	20
Requestor Location	Mr. Steven Condamine Département de neurosciences Université de Montréal C.P. 6128, Succ. Centre-ville Montreal, H3C3J7 France Attn: Mr. Steven Condamine
Publisher Tax ID	EU826007151
Total	0.00 CAD
Terms and Conditions	

Questions? customercare@copyright.com or +1-855-239-3415 (toll free in the US) or +1-978-646-2777.

Click here to download Supplemental File (Figures, Permissions, etc.) supplementary methods.docx

The angular difference of an astrocytic network is used to determine whether its preferential orientation is towards the center of the nucleus of interest. For each network a straight line (black line in Figure 5) was drawn from the patched astrocyte (P, black dot in Figure 5) to the center of the theoretical nucleus of interest. In this case, as only the dorsal half of NVsnpr is of interest, the center was defined as the intersection of a line from the 50% lateromedial axis and a line from 25% dorsoventral axis of the bounding rectangle (C, blue dot Figure 5). The angular difference (α, Figure 5) is the angle between the main vector of preferential direction of the network (PD, red line, Figure 5) and the line connecting P to C. To calculate the angular difference, use the Al-Kashi theorem into the triangle PDC (inset of Figure 5). This theorem gives the following equation:

$$d^2 = c^2 + p^2 - 2cp\cos\alpha$$

Where d is the length of [PC], c is the length of [PD] and p the length of [DC].

To calculate the angular difference, the Al-Kashi theorem was used with the following equation:

$$\alpha = \cos^{-1}(d^2 + p^2 - \frac{c^2}{2cd})$$